# Accounts

## Molecular Design of Prostaglandin Probes in Brain Research: High, Specific Binding to a Novel Prostacyclin Receptor in the Central Nervous System

**Masaaki Suzuki,* Ryoji Noyori,† Bengt Långström,†† and Yasuyoshi Watanabe†††**

Department of Biomolecular Science, Faculty of Engineering, Gifu University, Gifu 501-1193

†Department of Chemistry and Research Center for Material Science, Nagoya University, Nagoya 464-8602

††Department of Organic Chemistry, Institute of Chemistry, and Uppsala University PET Centre, UAS, S-751 85 Uppsala, Sweden

†††Department of Neuroscience, Osaka Bioscience Institute, 6-2-4 Furuedai, Suita, Osaka 565-0874 and Department of Physiology, Medical School, Osaka City University, 1-4-3 Asahimachi, Abeno-ku, Osaka 545-8585

(Received December 3, 1999)

Molecular design to develop a stable biochemical probe for a study of the role of prostacyclin ($PGI_2$) in the brain led to the discovery of (15*R*)-16-*m*-tolyl-17,18,19,20-tetranorisocarbacylin (referred to as 15*R*-TIC), that selectively bind to a novel $PGI_2$ receptor, $IP_2$, expressed in the central nervous system (CNS). This artificial prostaglandin with the 15*R* configuration exhibits high binding affinity for the $IP_2$ receptor in the thalamus ($IC_{50}$ = 32 nM) and weak affinity for the peripheral-type $PGI_2$ receptor, $IP_1$, in the NTS ($IC_{50}$ = 1.2 μM). The length of the $\omega$ side-chain and the position of the methyl substituent on the aromatic ring strongly influence the binding characteristics. The features of the $IP_2$ receptor were elucidated by quantitative mapping, specificity studies, and Scatchard analysis, as well as by a study using knockout mice with a tritium-labeled 15*R*-TIC and related radioligands. In order to conduct in vivo PET studies, a rapid methylation reaction using methyl iodide and an excess amount of an aryltributylstannane has been developed. This has successfully been applied to the synthesis of short-lived $^{11}$C-incorporated PET tracers, 15*R*-[$^{11}$C]TIC and its methyl ester. The PET experiments accomplished the imaging of the $IP_2$ receptor in the brain of living rhesus monkeys through intravenous administration. The elimination of the C(15) chirality results in 15-deoxy-TIC with ten-fold higher affinity and selectivity for the $IP_2$ receptor than original 15*R*-TIC. Neither 15*R*-TIC nor 15-deoxy-TIC inhibit platelets aggregation, up to 400 nM, while $PGI_2$ derivatives which bind with the $IP_1$ receptor show a very potent inhibitory effect at a several nM level. Notably, these artificial CNS-specific $PGI_2$ ligands, like the unstable natural $PGI_2$ itself, prevent the apoptotic cell death of hippocampal neurons induced under high (50%) oxygen atmosphere and by xanthine and xanthine oxidase or serum deprivation. The difference in the binding potency between 15*R*-TIC and 15-deoxy-TIC for the $IP_2$ receptor correlates well with the extent of the prevention of the neuronal cell death ($IC_{50}$ values of 300 and 30 nM, respectively, under high oxygen atmosphere). 15*R*-TIC protects CA1 pyramidal neurons against ischemic damage in gerbils. Thus the designed TICs have neuronal survival-promoting activity both in vitro and in vivo, providing the possibility as a new type of chemotherapeutic agents for applications in neurodegeneration.

Prostaglandins (PGs) exhibit diverse biological activities controlling a wide range of physiological functions in the circulatory, reproductive, respiratory, and digestive systems.[1] PGs are also involved in vital defense processes such as inflammation, tissue repair, and immune response.[1] These activities emerge via signal transduction initiated by the interaction of PGs with their cell-surface receptors. The amino acid sequences of eight typical PG receptors such as DP, FP, IP, TP, and four subtypes of EP have so far been elucidated and all of the receptors are assumed to belong to the G-protein-coupled rhodopsin-type cell membrane receptor superfamily.[2] The PG science has been growing by adding new subjects connecting with molecular mechanisms of the antineoplastic and antiviral actions of enone and cross-conjugated dienone PGs[3] and the involvement of these in osteogenesis,[4] adipogenesis,[5] induction of stress-gene expression,[6] and promotion of neurite outgrowth and regeneration,[7] in addition to the drug resistance mechanisms associated with MRP/GSX pump.[3,8] The biological actions of such enone-type PGs are considered to occur by the interaction with some targets inside of the cells

including nuclear receptors.[3,6,7]

The role of PGs in brain function has also attracted intense attention in recent years,[6,9] because the neuroscience research is expected to be a leading criterion of the PG life science in the next generation. The biological activities of PGs in the central nervous system are represented by those of $PGD_2$ (**1**) and $PGE_2$ (**2**) (Chart 1).[9a,10] $PGD_2$ exhibits the sleep-inducing effect, hypothermia, and inhibition of the release of luterining hormone-releasing hormone (LH-RH).[10,11] These effects are contrasted to those of $PGE_2$ such as promotion of wakefulness, hyperthermia, and acceleration of LH-RH release. The PGD synthase is secreted into the cerebrospinal fluid as a $\beta$-trace to produce $PGD_2$, which is then bound to the DP receptor on the surface of the ventro-medial region of the rostral basal forebrain.[12] The signal induced by this binding is considered to be transmitted into the brain parenchyma by adenosine via an adenosine $A_{2a}$ receptor to exhibit the sleep-inducing effect.[12] In situ hybridization studies demonstrated that a type of PG endoperoxide synthase (COX-2) is induced during endotoxin or cytokine-induced hyperthermia in vascular endothelial cells in brain.[13] Further, the $EP_3$ receptor has high expression in the small neurons of the dosal root ganglion,[14] suggesting the involvement of this receptor in $PGE_2$-mediated hyperalgesia.[9c] Here, we have been interested in the biological actions of prostacyclin ($PGI_2$, **3**) and its receptor function in the brain. This paper is mainly focused on our recent study on this chemistry/biochemistry/medicine interdisciplinary subject.

## Peripheral-Type Prostacyclin Receptor

$PGI_2$ (**3**) is a potent vasodilator and plays an important role in the circulatory system through both vasodilating and antithrombotic actions.[1,15] It activates adenylate cyclase in platelets, vascular smooth muscle, NCB-20 and mastocytoma P-815 cells, but its low stability,[16] the low receptor concentration in cell membranes, and the lack of a suitable biochemical probe prevented the identification of the receptor for a long time.[17] In this context, we succeeded in designing an efficient photoaffinity probe for the $PGI_2$ receptor, 19-(3-azidophenyl)-20-norisocarbacyclin (**4**), referred to as APNIC,[17] based on the structural modification of isocarbacyclin (**5**), a stable $PGI_2$ analogue.[18] APNIC (**4**) exhibited the specificity and high affinity for the $PGI_2$ receptor in the peripheral systems with a 50% inhibitory concentration ($IC_{50}$) of 3 nM (mastocytoma P-815 cells) and also acted as a $PGI_2$ agonist. The potency of **4** for the activation of adenyl-

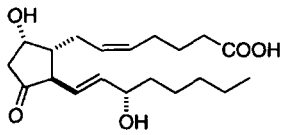


**1**, $PGD_2$

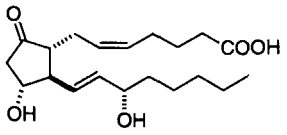


**2**, $PGE_2$

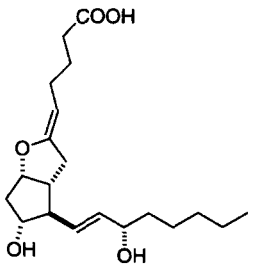


**3**, $PGI_2$

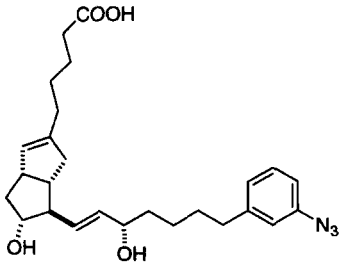


**4**, APNIC

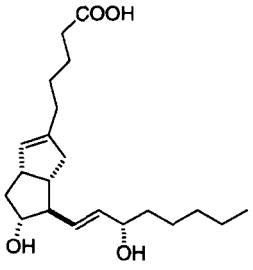


**5**, isocarbacyclin

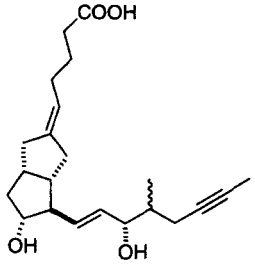


**6**, iloprost

Chart 1.

ate cyclase was found to be 70% of that of iloprost (**6**),[19] and its aggregation-inhibiting activity to rabbit platelets was one-fifth of that of **5**. The photoaffinity labeling experiment with a tritium-labeled APNIC (**7**) as the radio ligand allowed the identification of $PGI_2$ receptor proteins of approximately 43, 45, and 52 kD, for mast cells, porcine platelets, and human platelets, respectively (Chart 2).[17] Later, the cDNA cloning of rat and human $PGI_2$ receptors was also established by a Kyoto University group.[20]

Some earlier observations suggested that $PGI_2$ (**3**) would have neuromodulatory actions in the brain as well:[9a,9b,21] (1) $PGI_2$ is formed in rat and rabbit brain homogenate; (2) 6-Oxo-$PGF_{1\alpha}$ (**8**), a stable $PGI_2$ metabolite, is detectable not only in the postmortem human brain but also in the brain after convulsions;[21a] (3) Norepinephrine stimulates the production of $PGI_2$ in sympathetic postganglionic neurons;[21c,21d] (4) $PGI_2$ improves neuronal damage after experimental ischemia.[22] However, it has not been confirmed whether the last effect is a specific function of $PGI_2$ or not, because such protection may occur also by its beneficial effect on cerebral circulation as a vasodilator. In any case, the extreme chemical and metabolic instability of endogenous ligand $PGI_2$ (**3**) (half-life ($t_{1/2}$) < 5 min at pH 7.4),[16] causing ready hydrolysis of the enol ether moiety to give **8**, has hampered further detailed assessment of the role of **3** in the brain using the natural substance *per se*.

The existence and localization of the $PGI_2$ receptor in the rat brain and spinal cord were examined by in vitro autoradiography using [$^3$H]iloprost (**9**)[19] ($^3$H-labeled **6**), a highly specific and stable agonist for the $PGI_2$ receptor. The results indicated that the density of specific binding sites for iloprost is generally high in four regions of the lower brain stem, namely, the medial and commissural subnuclei of the nucleus tractus solitarius (NTS), the area postrema, superficial layers of the spinal trigeminal nucleus caudalis, and dorsal horn.[23] $PGE_2$ (**2**)-binding sites are also abundant in the NTS, spinal trigeminal nucleus caudalis, and dorsal horn, but these binding sites are clearly different from those for iloprost (**6**),[19] presumably serving a different function.[23] Iloprost (**6**) exerts a variety of actions associated with the central nervous system, such as sedative, anti-convulsive, anti-hypoxic, and synchronization of electroencephalogram.[24] Ganglionectomy and nerve ligation experiments showed that the $PGI_2$ receptor for **9** in caudal medulla such as the NTS is produced in nodose ganglia and then transported to the central terminus of the primary sensory afferents by an axonal flow as

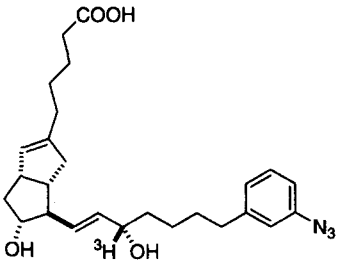


**7**, [$^3$H]APNIC

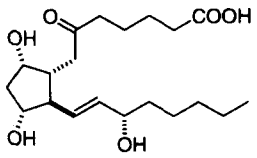


**8**, 6-oxo-$PGF_{1\alpha}$

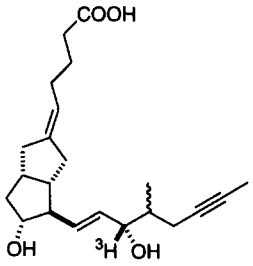


**9**, [$^3$H]iloprost

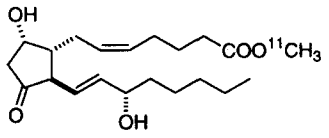


**10**, $PGD_2$ [$^{11}$C]methyl ester

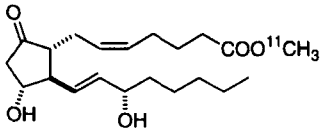


**11**, $PGE_2$ [$^{11}$C]methyl ester

Chart 2.

well as to their peripheral terminals (Fig. 1).[23] Further, in situ hybridization for a cloned peripheral-type $PGI_2$ receptor in the brain (a PNS-type $PGI_2$ receptor) showed no significant signals in the rostral regions of the brain (such as hippocampus, cerebral cortex, thalamus, striatum, or septum) but did show a high density of signals in sensory ganglia.[25] We have been intrigued by exploring a neuronal $PGI_2$ receptor that is specifically expressed in rostral regions in the brain through creation of efficient biochemical probes.

### Toward Biochemical Probes for a $PGI_2$ Receptor Specifically Expressed in the Central Nervous System

Precise analysis of the role of $PGI_2$ (**3**) in the brain requires the development of stable PGs as specific molecular probes capable of sharply discriminating its action in the rostral and peripheral portions in the central nervous system (CNS). In addition, such specific receptor ligands should be useful not only for in vitro analysis but also for in vivo investigations of living brains, including a human brain as a final goal. Accordingly, we set up the research plan for designing of biochemical probes to meet these requirements.

For imaging of the living human brain, there are several noninvasive methods such as X-ray computed tomography (X-ray CT), magnetoencephalography (MEG), magnetic resonance imaging (MRI) including functional MRI (fMRI), and positron emission tomography (PET) available as diagnostic techniques. Of these, PET would be the most appropriate because this technique allows identification of a target molecule such as an enzyme or a receptor using a designed radiolabeled ligand molecule at a subfemtomole-level low-concentration in the living brain, the study of metabolism and pharmacokinetics of drugs, and the related molecular level investigation.[26] These features are entirely different from those of X-ray CT and MRI techniques, which are mainly focused on morphological (anatomical) information of the brain. Fortunately, an international joint research program[27] provided us with an opportunity to develop $^{11}C$-incorporated PGs as biochemical probes, in which the use of [$^{11}C$]methyl iodide, a readily available synthetic precursor at the Uppsala University PET Centre, was the key in the incorporation of an [$^{11}C$]methyl group at an appropriate position in the PG structure. Although some biological works using $PGD_2$ and $PGE_2$ [$^{11}C$]methyl esters, **10** and **11**, had preceded,[28] the conclusions of these studies would not be reliable because such PG compounds generally exhibit very low affinity for the corresponding receptors and also readily undergo hydrolysis by an enzyme to liberate [$^{11}C$]methanol.[28] Thus we decided to incorporate an $^{11}CH_3$ group in the tolyl group at a terminal of the ω side-chain unit (Scheme 1). This idea originated from our long-term experience of organometallic chemistry (see later section) together with the well-known mechanism of PG metabolism by a P450 enzyme. The presence of an aromatic group in the side chain must prevent the oxidative biodegradation, hopefully with retention of a high receptor affinity.[29]

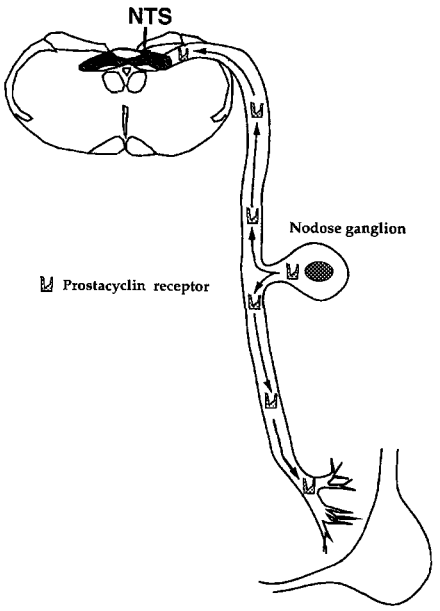


Fig. 1. The $PGI_2$ receptor with high affinity for [$^3H$]iloprost (**9**) is produced in nodose ganglia and then transported to caudal medulla as the presynaptic part of the central terminals of the primary sensory neurons by axonal flow.

**Turning Point: Discovery of 15*R*-TIC, a Stable Ligand for a CNS-Specific $PGI_2$ Receptor in the Brain. (1) Identification of the Novel $PGI_2$ Receptor ($IP_2$) Specifically Expressed in the Central Nervous System.** Our research after choosing isocarbacyclin (**5**)[18] as a lead compound continued in the dark for a long time; finally, two very fortunate results led to a breakthrough. The first was the finding that isocarbacyclin (**5**) and iloprost (**6**)[19] exhibited different distribution patterns for the $PGI_2$ receptor in the brain.[30] Thus, when [$^3H$]isocarbacyclin (**12**)[31] ($^3H$-labeled **5**) was preliminarily used in the autoradiographic study instead of [$^3H$]iloprost (**9**), it showed a binding potency much higher than that of **9** in the thalamus and cerebral cortex (Chart 3). Both ligands, however, showed comparable binding in some regions of the medulla and spinal cord, suggesting the existence of several (at least two) distinct $PGI_2$ receptors in the brain.[30] Secondly, we succeeded in designing a specific ligand, (15*R*)-16-*m*-tolyl-17,18,19,20-tetranorisocarbacyclin (**13**), referred to as 15*R*-TIC,[32] according to a synthetic plan

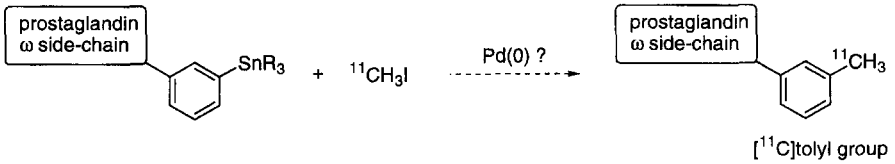


Scheme 1. Plan for $^{11}CH_3$-incorporation into the PG ω side-chain by the Stille reaction.

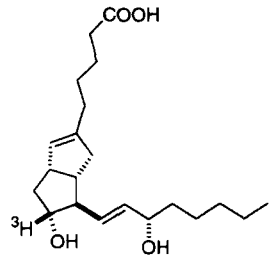


**12**, [$^3$H]isocarbacyclin

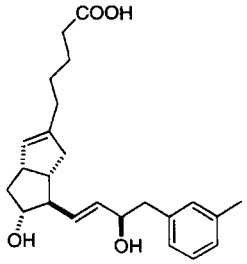


**13**, 15*R*-TIC

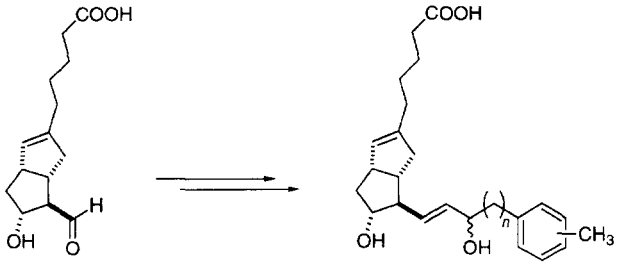


Scheme 2. Structural modification of the $\omega$ side-chain.

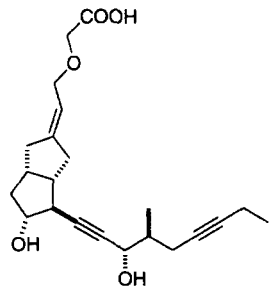


**14**, cicaprost

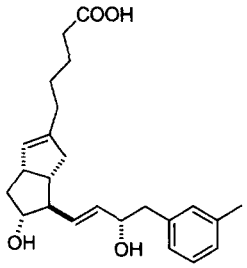


**15**, 15*S*-TIC

Chart 3.

in Scheme 2, which exhibits a high binding affinity and selectivity for the novel $PGI_2$ receptor, specifically expressed in the rostral regions in the brain. This finding clearly discriminated the dual binding patterns of isocarbacyclin (**5**). The binding specificities of the three selected stable $PGI_2$ analogues are compared in Fig. 2. The binding assay of these compounds was conducted for $PGI_2$ receptor in frozen tissue sections of the brain using [$^3$H]isocarbacyclin (**12**)[31] as a radioligand. The thalamus (plots A) and the NTS (plots B) are representatives of the central and peripheral nervous systems, respectively. The 50% inhibitory concentrations of the binding ($IC_{50}$) were determined by the degree of the displacement of 10 nM [$^3$H]isocarbacyclin (**12**) (1 M = 1 mol dm$^{-3}$) bound to the receptor by nonradioactive compounds. As shown in Fig. 2, 15*R*-TIC (**13**) exhibited a sufficiently high binding affinity for the CNS-specific $PGI_2$ receptor in the thalamus ($IC_{50}$ = 31 nM) but showed a binding with the PNS-type $PGI_2$ receptor in the NTS ($IC_{50}$ = 1.2 μM). Such a binding profile of **13** was contrasted markedly with that of cicaprost (**14**),[33] a stable $PGI_2$ agonist belonging to the iloprost family, which showed a high binding affinity and selectivity for the PNS-type $PGI_2$ receptor in the NTS ($IC_{50}$ = 30 nM). Isocarbacyclin (**5**), the lead compound, exhibited a high binding affinity for both receptors with $IC_{50}$ values of 31 and 23 nM in the thalamus and NTS, respectively. The 15*S*-TIC (**15**) showed a slightly lower binding ($IC_{50}$ = 38 nM) for the CNS-specific $PGI_2$ receptor in the thalamus than **13**, while maintaining a strong binding affinity ($IC_{50}$ = 32 nM) for the PNS-type $PGI_2$ receptor in the NTS similar to those of **5**. Thus **15** would serve as a good probe compound for the PNS-type $PGI_2$ receptor in the brain, instead of **5** which has the same 15*S* stereochemistry.[34] Other 15-hydroxy-type tolylisocarbacyclins showed weaker binding affinity for the CNS-specific $PGI_2$ receptor in the thalamus.

The structure/binding affinity relationships of tolylisocarbacyclins for $PGI_2$ receptors are of much interest. The chain length of the $\omega$ side-chain as well as the position of a methyl substituent on the aromatic ring influences the binding affinity to a great extent (Fig. 3). The binding affinity

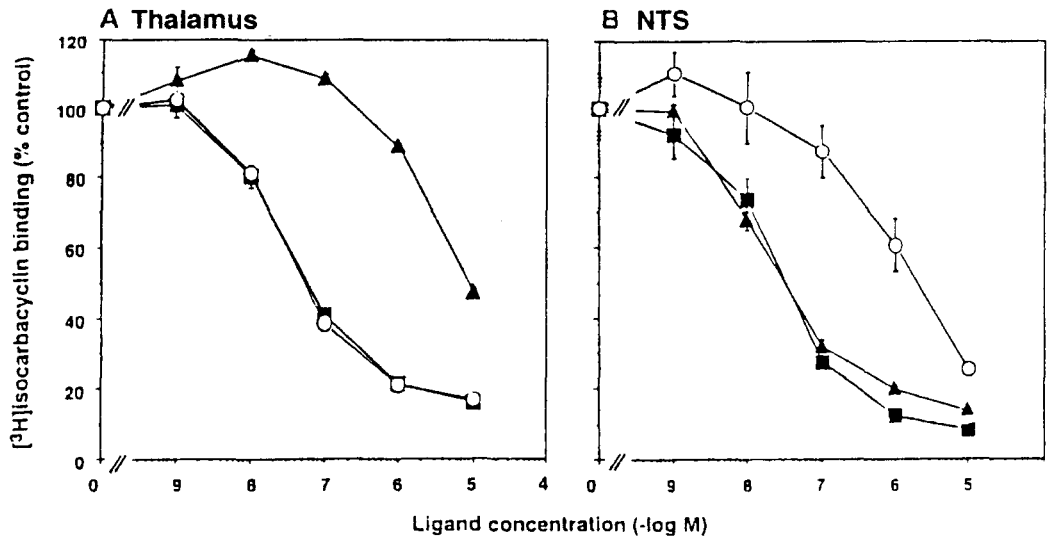


Fig. 2. Displacement of 10 nM [$^3$H]isocarbacyclin (**12**) binding by nonradioactive 15*R*-TIC (**13**) (○), isocarbacyclin (**5**) (■), and cicaprost (**14**) (▲) in thalamus (**A**) and the NTS (**B**) of rat frozen sections of the brain.

for the PNS-type $PGI_2$ receptor in the NTS increased in the order of:

$$16\text{-}m\ (n=1) < 17\text{-}p\ (n=2), 19\text{-}p\ (n=4) < 17\text{-}m\ (n=2) < 19\text{-}m\ (n=4).$$

On the other hand, the binding affinity for the CNS-specific $PGI_2$ receptor in the thalamus increased in the order of:

$$19\text{-}m, 19\text{-}p\ (n=4) << 17\text{-}p\ (n=2) < 17\text{-}m\ (n=2) < 16\text{-}m\ (n=1).$$

Thus, the receptor in the NTS favors longer side-chain derivatives, while the receptor in the thalamus matches more with the shorter chain analogues.[32] In both cases, the *meta*-methyl substituent on the aromatic ring was preferred. Overall, 15*R*-TIC (**13**) exhibits the highest binding affinity for the CNS-specific $PGI_2$ receptor in the thalamus. It is worth noting that the binding tendency obtained for the PNS-type $PGI_2$ receptor in the NTS is consistent with the behavior of azidophenylisocarbacyclins for the $PGI_2$ receptor in mast cells and platelets as peripheral systems shown in our previous study.[17] On the basis of such different binding characteristics for $PGI_2$ receptors in the brain in combination with accumulated biological properties described in later sections, we proposed to designate $IP_1$ and $IP_2$ for peripheral-type and CNS-specific $PGI_2$ receptors, respectively.[30]

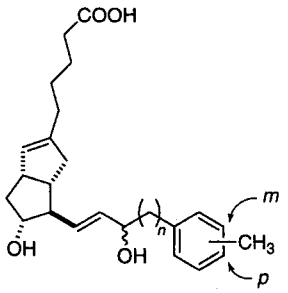


Fig. 3. Importance of the chain length and the position of a methyl substituent on the aromatic ring for the binding specificity.

**(2) Synthesis of 15*R*-TIC.** 15*R*-TIC (**13**)[32] was synthesized based on the structural modification of the $\omega$ side-chain of isocarbacyclin (**5**),[18] shown in Scheme 3. The starting aldehyde intermediate **16** was available by several methods, including our three-component coupling PG synthesis.[17a,35,36] Thus, the aldehyde **16** was first condensed with the phosphonate **17** under basic conditions to afford the enone **18** in 96% yield. Then, regioselective 1,2-reduction of the conjugated enone with sodium borohydride in the presence of cerium(III) chloride gave the diol **19**, a 1 : 1 mixture of stereoisomers at C(15), in quantitative yield. The stereoisomers were separated by conventional silica-gel column chromatography to give the stereochemically pure *R* and *S* alcohols, (*R*)-**19** and (*S*)-**19** (each in 50% yield), as the less and more polar materials, respectively. Finally, alkaline hydrolysis of (*R*)-**19** and (*S*)-**19** led to the corresponding tolylisocarbacyclin derivatives **13** and **15** in quantitative yields.[32] Other tolylisocarbacyclin derivatives for the binding assay were also synthesized by a similar method, using the corresponding Horner–Emmons reagents. Here, the potent affinity of the 15*R*-configurated alcohol, 15*R*-TIC (**13**), is surprising because the configuration of this hydroxy-bearing chiral center in hormonal PGs is generally *S*. 15*S* PG derivatives are usually known to be more polar than the corresponding 15*R* derivatives, showing smaller $R_f$ values on TLC analysis. In order to confirm such 15*R* unnatural stereochemistry of **13**, the absolute configurations at C(15) of the tolylisocarbacyclin derivatives, **13** and **15**, were de-

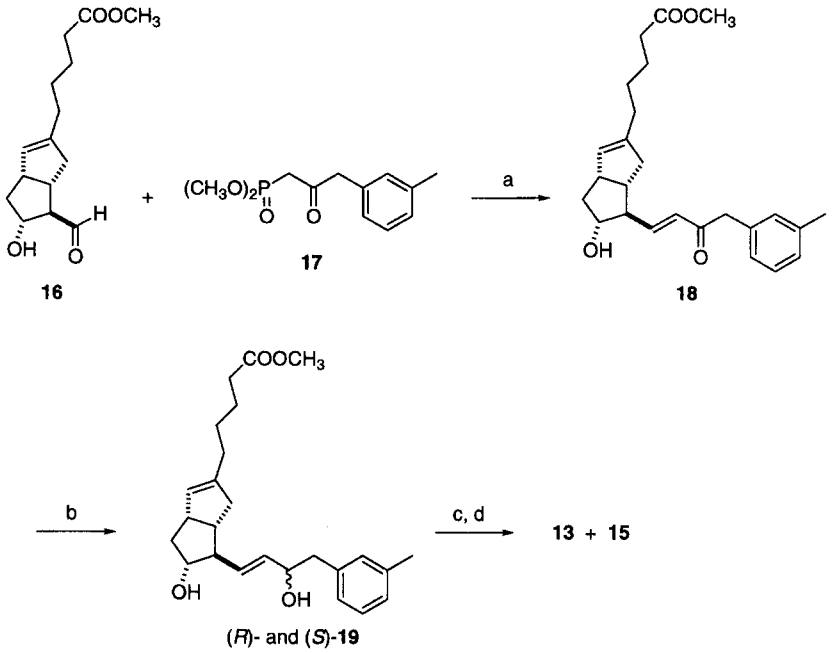


Scheme 3. Synthesis of optically pure tolylisocarbacyclins. a) NaH, DME, 96%.; b) $NaBH_4$, $CeCl_3$, $CH_3OH$, quant.; c) separation of 15-epimers giving (*R*)-**19** (less polar) and (*S*)-**19** (more polar); d) aq LiOH, quant. (2 steps).

termined carefully by unambiguous chemical correlation of the degradation product from 15*S*-TIC methyl ester ((*S*)-**19**) with the bis(MTPA) ester ((2*S*)-**20**) derived from the stereodefined glycerol derivative (2*S*)-**21**, as outlined in Scheme 4. Thus selective masking of the double bond in the five-membered ring of (*S*)-**19** by intramolecular iodoetherification, followed by esterification of the C(15) hydroxy group with (*S*)-$\alpha$-methoxy-$\alpha$-(trifluoromethyl)phenylacetyl chloride ((*S*)-MTPA chloride), provided the MTPA ester **22**. Oxidative cleavage of the olefinic bond in the $\omega$ side-chain, reduction of the resulting aldehyde to the alcohol, and MTPA esterification gave the tolyl-containing bis(MTPA) ester (2*S*)-**20** and the tricyclic residue. The stereodefined ester (2*S*)-**20** was prepared independently from the optically pure glycerol derivative (2*S*)-**21** by oxidation to an aldehyde, reaction with a tolyl Grignard reagent, and then by Barton deoxygenation of the resulting alcohol. A mixture of (2*R*)- and (2*S*)-**20** was also prepared via the racemic **21**. HPLC analysis of these authentic samples indicated that the retention time of **20** obtained by degradation of the isocarbacyclin derivative (*S*)-**19** is identical with that of (2*S*)-**20**. Thus it is concluded that the C(15) stereocenter of **15** has the *S* configuration and that **13** possesses the *R* configuration.[32]

**Quantitative Mapping, Specificity Studies, and Scatchard Analysis of the CNS-Specific $PGI_2$ Receptor ($IP_2$) in Rat Brain.** **(1) Mapping of 15*R*-TIC Binding Sites.**[37] Autoradiography was used to investigate the localization of 15*R*-TIC binding sites using 15*R*-[$^3$H]TIC (**23**) ([$^3$H]-labeled **13**) with a number of coronal sections of rat brain. The result indicated that 15*R*-[$^3$H]TIC binding was high in most of the thalamic regions, limbic structures, and some parts of the cortical regions (Fig. 4). The highest binding was shown in the dorsal part of lateral septal nucleus, together with more precise analysis of the ligand distribution: (in the thalamus) high in the centromedian, paraventricular, rhomboid, and medial geniculate nuclei, followed by dorsolateral geniculate nucleus and anterodorsal/anteroventral nuclei; (in the cortical regions) especially high in the entorhinal, piriform, and perirhinal cortices, in this order, followed by occipital, frontal, and anterior cingulate cortices; (in other regions) high in the anterior olfactory nucleus, in the bed nucleus of accessory olfactory tract, in the posterior cortical amygdaloid nucleus, in the ventral part of caudoputamen, and in the dorsal cochlear nucleus in the pons. Further, the dentate gyrus and CA1 and CA3 regions of the hippocampus showed relatively high density.

**(2) Binding Specificity.**[37] In the thalamus, 15*R*-TIC (**13**) displaced 15*R*-[$^3$H]TIC binding most efficiently ($IC_{50}$ = ca. 10 nM), followed by 15*S*-TIC (**15**) and isocarbacyclin (**5**, 15*S*). Likewise, 15*S*-[$^3$H]TIC (**24**) binding was displaced by 15*R*-TIC (**13**), isocarbacyclin (**5**, 15*S*), and then 15*S*-TIC (**15**) in this order. In contrast, $PGE_1$, which has comparably high affinity for the $IP_1$ receptor in the NTS, showed a low affinity for the $IP_2$ receptor. The affinity of $PGE_1$ and $PGE_2$ was two orders of magnitude less. $PGD_2$ and $PGF_{2\alpha}$ showed even less affinity.

**(3) The Scatchard Analysis.**[37] We performed the Scatchard plot analysis to further characterize $IP_1$ and $IP_2$ receptors. *Two components* with high and medium-high affinity were observed with 15*R*-[$^3$H]TIC (**23**) used in the thalamus and striatum (A and B in Fig. 5). The high-affinity sites for **23** in the thalamus showed a $K_d$ value of 0.94 nM and a $B_{max}$ value of 79 fmol/mg tissue, and the medium high-affinity sites, showed a $K_d$ of 30 nM and a $B_{max}$ of 380 fmol/mg tissue (Table 1). In the striatum, high-affinity sites for **23** showed a $K_d$ of 0.54 nM and a $B_{max}$ of 71 fmol/mg

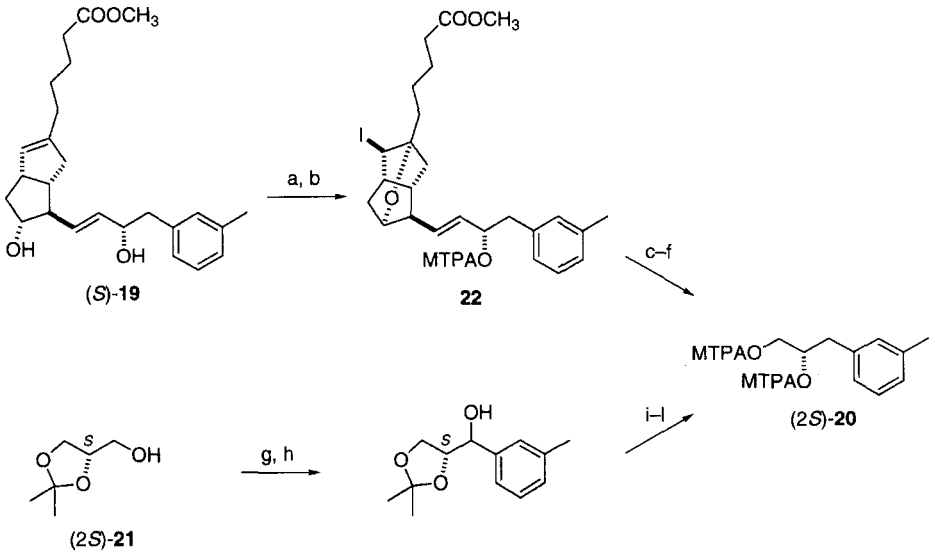


Scheme 4. Determination of the C(15) stereochemistry. a) $I_2$, $CH_3OH/H_2O$ (3/1), 89%; b) (*S*)-MTPACl, pyridine, 92%; c) $OsO_4$, pyridine; d) $NaIO_4$, THF/ether/$H_2O$ (2/1/1); e) $NaBH_4$, $CH_3OH$; f) (*S*)-MTPACl, pyridine, 20% overall yield from **22**; g) PCC, $CH_2Cl_2$; h) *m*-$CH_3C_6H_4MgCl$, ether; i) NaH, THF, then $CS_2$, $CH_3I$, 98%; j) *n*-$(C_4H_9)_3SnH$, toluene, reflux, 66%; k) $CF_3COOH$, THF/$H_2O$ (4/1); l) (*S*)-MTPACl, pyridine.

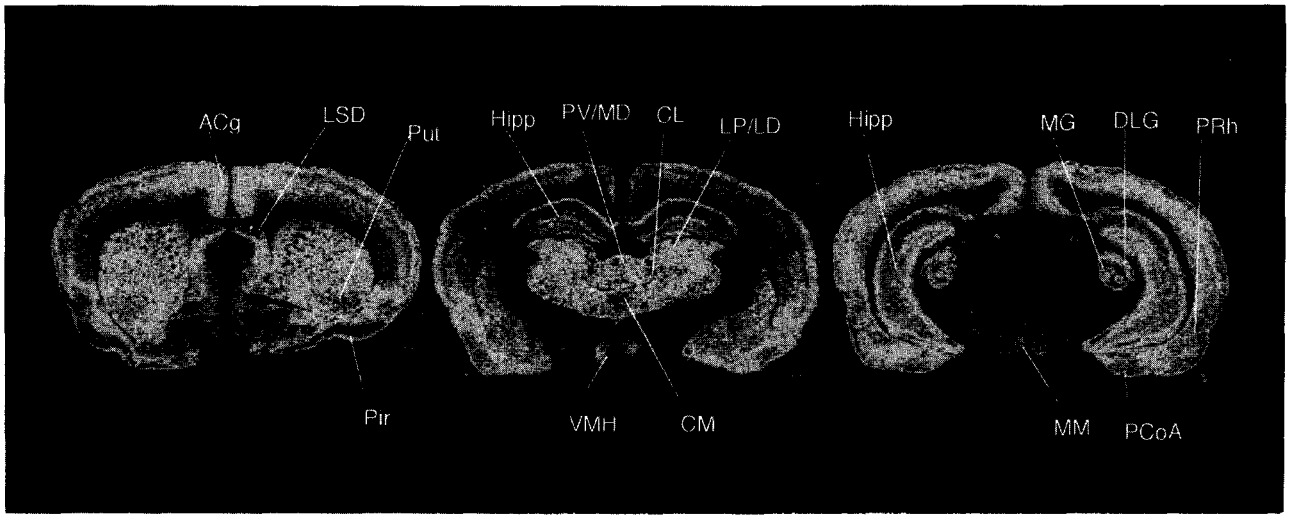


Fig. 4. Autoradiography of the binding of 15*R*-[$^3$H]TIC (**23**) in coronal sections in rat brain. ACg, anterior cingulate cortex; LSD, lateral septal nu., dorsal; Put, putamen; Pir, piriform cortex; Hipp, hippocampus; PV/MD, paraventricular thalamic nu./mediodorsal thalamic nu.; CL, centrolateral thalamic nu.; LP/LD, lateral posterior thalamic nu./laterodorsal thalamic nu.; VMH, ventromedial hypothalamic nu.; CM, central medial thalamic nu.; MG, medial geniculate nu.; DLG, dorsal lateral geniculate nu.; PRh, perirhinal cortex.; MM, medial mammillary nu.; PCoA, posterior amygdaloid nu.

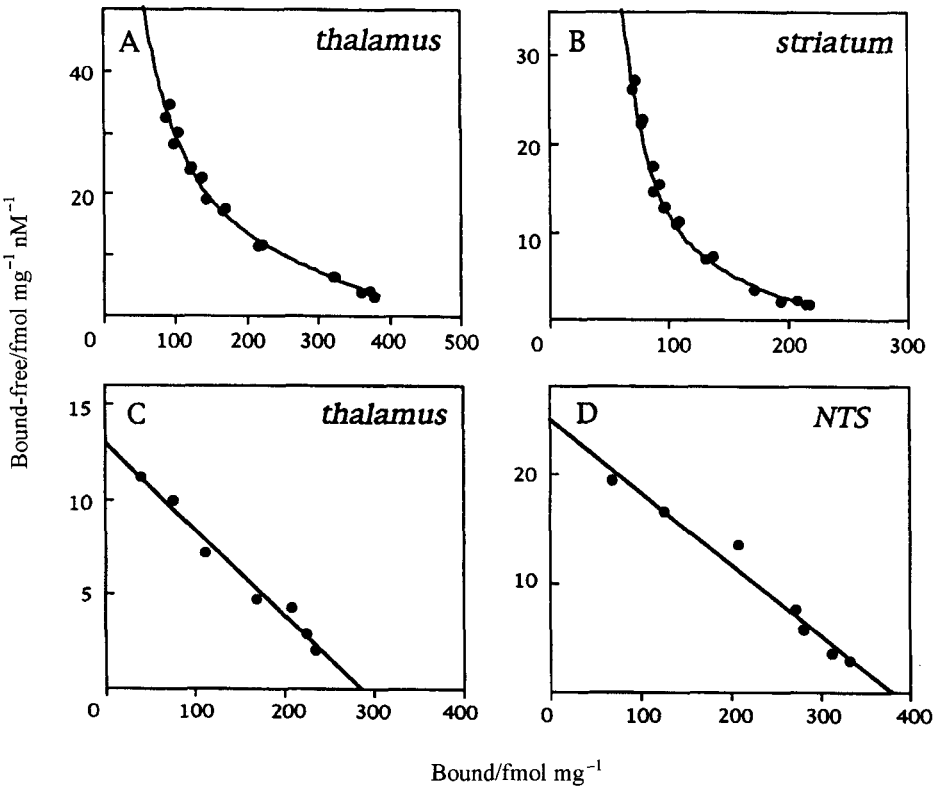


Fig. 5. Scatchard analysis of 15*R*-[$^3$H]TIC (**23**) and 15*S*-[$^3$H]TIC (**24**) in rat brain sections.

tissue, and the medium high-affinity sites, showed a $K_d$ of 37 nM and a $B_{max}$ of 185 fmol/mg tissue (Chart 4). In contrast, 15*S*-[$^3$H]TIC (**24**) indicated a *single component* of binding with its $K_d$ and $B_{max}$ values of 22 nM and 280 fmol/mg tissue, in the thalamus, and 15 nM and 380 fmol/mg tissue, in the NTS (C and D in Fig. 5). Such 15*S*-[$^3$H]TIC binding was compatible with binding of [$^3$H]isocarbacyclin (**12**). Our hemilesion experiments with kainate in the rat striatum revealed that the CNS-specific $PGI_2$ receptor was expressed mainly in neurons, but not in the presynaptic terminals of afferents or glial cells.[30] Thus we obtained valuable information by the in vitro autoradiographic analysis of brain slices, strengthening the view that a different subtype of prostacyclin receptor is expressed in the CNS. In addition, our binding experiments using $IP_1$-knockout mice[38] clearly demonstrated the independent expression of the $IP_2$ receptor

Table 1. Data of the Scatchard Plot Analyses in Rat Brain Sections

| | NTS | Thalamus | Striatum |
|---|---|---|---|
| 15*R*-TIC (**13**) | — | 0.94 nM | 0.54 nM |
| | — | 79 fmol/mg | 71 fmol/mg |
| | — | 30 nM | 37 nM |
| | — | 380 fmol/mg | 185 fmol/mg |
| 15*S*-TIC (**15**) | 15 nM | 22 nM | — |
| | 380 fmol/mg | 280 fmol/mg | — |
| Isocarbacyclin (**5**) | 3.9 nM | 7.8 nM | 8.9 nM |
| | 199 fmol/mg | 230 fmol/mg | 165 fmol/mg |
| Iloprost (**6**) | 6.8 nM | 159 nM | — |
| | 194 fmol/mg | 163 fmol/mg | — |

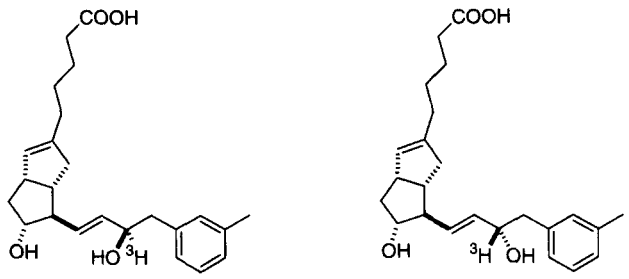


**23**, 15*R*-[$^3$H]TIC **24**, 15*S*-[$^3$H]TIC

Chart 4.

in the CNS of such knockout mice.[39]

## In Vivo Imaging

The principle of the PET imaging using $^{11}$C as the radionuclide is illustrated in Fig. 6. $^{11}$C undergoes $\beta^+$ decay with a half-life of 20.3 min, yielding $^{11}$B as the stable nuclide. A positron (positively charged electron, $e^+$) ejected by this process collides with an electron within a short distance in tissue to produce two $\gamma$-ray photons of 511 keV that travel in opposite directions. The photons produced by the annihilation event are detected by a pair of opposing scintillation detectors and then the data are fed to a computer that reconstructs the spatial distribution of the produced decay events. The fate of an $^{11}$C-incorporated compound can be imaged quantitatively with high sensitivity and high spatial resolution. Thus PET is used as a powerful scientific tool for in vivo studies on biochemical transformations and the movement of drugs in the human brain as well as other organs in the body with a very low radiation dose.[26,40] In general, the synthesis of a PET tracer for all practical purposes must be accomplished within 3 half-lives after the radionuclide is produced.

**(1) Realization of Rapid Methylation.**[41] The tolyl group in **13** is an obvious trigger component to create a radioligand including an $^{11}$C positron nuclide. It was expected that the $^{11}CH_3$ group could readily be introduced by the Stille reaction[42] using $^{11}CH_3I$, a frequently used precursor for $^{11}$C-labeled tracers. The Stille reaction would be useful for this purpose, because an organotin function is tolerant not only of most functional groups present in biomolecules but also of standard workup and purification conditions. Then, the incorporation of the short-lived $^{11}$C nuclide ($t_{1/2}$ = 20.3 min) might be accomplished at the final stage of the synthesis. However, there was little information on the Stille reaction with methyl iodide[43] in spite of a wide applicability to many $sp^2$ or allylic organic halides.[42] Actually, the trap of $^{11}CH_3I$ with tributylphenylstannane as a model was very sluggish,[44] hampering the incorporation of $^{11}$C into **13**. When trimethylphenylstannane was used, both phenyl and methyl moieties participated in the reaction, producing undesired $^{11}CH_3$-containing ethane as a by-product. As such, methylation under the standard Stille conditions was not viable, prompting us to develop a rapid coupling reaction.

Conditions for the synthesis of PET tracers are very different from those in ordinary organic syntheses, since time is a restricting parameter along with conventional parameters like chemical yield. In particular, the reaction is conducted using an extremely small amount of $^{11}CH_3I$. In addition, the reaction must be accomplished within several minutes to leave enough time for work-up and chromatographic purification, because of the short lifetime of the positron nuclide. Assuming such limited conditions, we set up the coupling reaction with the use of a large excess of tributylphenyl-

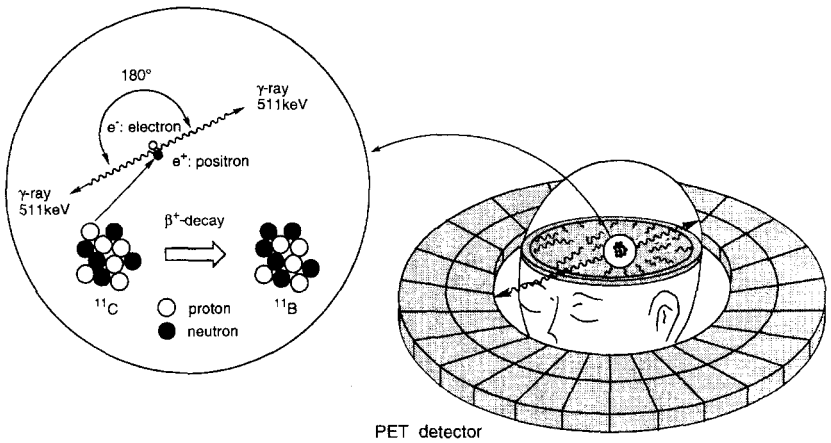


Fig. 6. Principle of the brain imaging by PET.

stannane relative to methyl iodide (> 40 : 1) and a short reaction time. As a consequence of extensive experimentation, as indicated in Table 2, the ultimate solution to the Stille methylation was provided by the stoichiometric use of a combined $[Pd\{P(o\text{-}CH_3C_6H_4)_3\}_2]/CuCl/K_2CO_3$ system in DMF at 60 °C for 5 min, giving toluene in 81% yield (Entry 11 in Table 2). The $Pd^0$ complex generated in situ from $[Pd_2(dba)_3]$ and $P(o\text{-}CH_3C_6H_4)_3$ (1 : 4) was found to be more effective (giving the desired product in 91% yield) than the performed complex (Entry 14 in Table 2). The reaction in DMF solvent was relatively tolerant of high-temperature conditions even in the absence of a Cu(I) salt and $K_2CO_3$. The reaction at 80 °C gave the coupling product in a moderate yield (63%) (Entry 10 in Table 2). In fact, the higher-temperature condition (130 °C) was applied to the real PET study on a monkey brain (see later section). Here, aryltributylstannanes appear to be more useful as trapping agents than aryltrimethylstannanes, because the unnecessary $^{11}CH_3/^{12}CH_3$ scrambling in the toluene is avoidable. The protocol using a Cu(I) salt and $K_2CO_3$ allowed controlled methylation of a variety of tributyltin derivatives of benzyl alcohol, anisole, thiophene, and furan.[41]

The coupling reaction between of methyl iodide and tributylphenylstannane proceeds presumably by the mechanism shown in Scheme 5. In the first step, methyl iodide undergoes oxidative addition to a $Pd^0$ species to generate the methyl-$Pd^{II}$ iodide **25** (Eq. 1). The $Pd^{II}$ complex **25** may then react directly with the phenyltin compound **26** to afford the (methyl)(phenyl)$Pd^{II}$ complex **28** (Eq. 3); its formation would, however, be facilitated by the phenylcopper compound **27** formed by prior Sn/Cu transmetallation (Eq. 2). Finally, toluene is formed by reductive elimination from the $Pd^{II}$ complex **28** (Eq. 4). The marked ligand effect of tri-*o*-tolylphosphine is attributed to its great bulkiness (cone angle = 194°, which is greater than that in tri-*t*-butylphosphine, 182°), which facilitates the generation of the coordinatively unsaturated $Pd^0$ and $Pd^{II}$ intermediates.[45] The substitution to give **28** and/or reductive elimination of toluene requires the formation of the tricoordinate $Pd^{II}$ complex. DMF may stabilize such Pd intermediates at high temperatures. The effect of $K_2CO_3$ remains unclear.

Thus we succeeded in the rapid methylation of aromatic organotin derivatives using methyl iodide, providing a firm basis for the synthesis of $^{11}C$-incorporated PET tracers. This new protocol also allows for ready isotope labeling, including $^{13}CH_3$- and $^{14}CH_3$-incorporated aromatic compounds. The applicability of this protocol was best demonstrated by the syntheses of the $^{11}C$-incorporated 15*R*-TIC and its methyl ester.

**(2) Synthesis of 15*R*-[$^{11}$C]TIC Methyl Ester[46] and Brain Imaging of a Living Monkey.**[47] In order to extend our in vitro study on the $IP_2$ receptor to the more important in vivo investigation in a living brain, the synthesis of an $^{11}C$-incorporated TIC derivative is crucially important. The requisite $^{11}C$-incorporated methyl iodide was prepared from [$^{11}$C]carbon dioxide via reaction with lithium aluminium hydride and subsequent reaction with hydroiodic acid according to the established method.[48] This process took only 6 min. Then, [$^{11}$C]methyl iodide was transferred to $[Pd_2(dba)_3]$ (1 μmol)/$P(o\text{-}CH_3C_6H_4)_3$ (4 μmol) in DMF (350 μl) followed by mixing with the tributyltin derivative **29** (1.4 μmol) (Chart 5).[49] Then the mixture was heated at 130 °C for 7

Table 2. Pd(0)-Mediated Coupling of Methyl Iodide with Excess Tributylphenylstannane

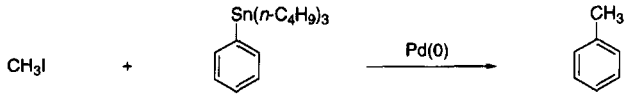


| Entry[a] | Pd(0) complex | Ligand | Pd : ligand Mol ratio | Additive[b] | Solvent | Time min | Temp °C | Toluene Yield/%[c] |
|---|---|---|---|---|---|---|---|---|
| 1 | $[Pd(PPh_3)_4]$ | — | — | — | DMSO | 30 | 40 | 0 |
| 2 | $[Pd(PPh_3)_4]$ | — | — | — | DMSO | 30 | 90 | 10 |
| 3 | $[Pd(PPh_3)_4]$ | — | — | $CuCl/K_2CO_3$ | THF | 5 | 40 | 20 |
| 4 | $[Pd(PPh_3)_4]$ | — | — | $CuCl/K_2CO_3$ | THF | 5 | 60 | 23 |
| 5 | $[Pd_2(dba)_3]$ | $AsPh_3$ | 1 : 2 | CuI | DMF | 5 | 60 | 0 |
| 6 | $[Pd_2(dba)_3CHCl_3]$ | $P(o\text{-}CH_3C_6H_4)_3$ | 1 : 2 | — | 1,4-Dioxane | 30 | 40 | 75 |
| 7 | $[Pd_2(dba)_3CHCl_3]$ | $P(o\text{-}CH_3C_6H_4)_3$ | 1 : 2 | — | DME | 30 | 40 | 76 |
| 8[d] | $[Pd_2(dba)_3CHCl_3]$ | $P(o\text{-}CH_3C_6H_4)_3$ | 1 : 2 | — | DME | 30 | 40 | 86 |
| 9 | $[Pd_2(dba)_3CHCl_3]$ | $P(o\text{-}CH_3C_6H_4)_3$ | 1 : 2 | — | DME | 5 | 80 | 41 |
| 10 | $[Pd_2(dba)_3]$ | $P(o\text{-}CH_3C_6H_4)_3$ | 1 : 2 | — | DMF | 5 | 80 | 63 |
| 11 | $[Pd\{P(o\text{-}CH_3C_6H_4)_3\}_2]$ | — | — | $CuCl/K_2CO_3$ | DMF | 5 | 60 | 81 |
| 12 | $[Pd_2(dba)_3]$ | $P(o\text{-}CH_3C_6H_4)_3$ | 1 : 2 | CuI | DMF | 5 | 60 | 3 |
| 13 | — | — | — | $CuCl/K_2CO_3$ | DMF | 5 | 60 | 0 |
| 14 | $[Pd_2(dba)_3]$ | $P(o\text{-}CH_3C_6H_4)_3$ | 1 : 2 | $CuCl/K_2CO_3$ | DMF | 5 | 60 | 91 |
| 15 | $[Pd_2(dba)_3]$ | $P(o\text{-}CH_3C_6H_4)_3$ | 1 : 2 | $CuBr/K_2CO_3$ | DMF | 5 | 60 | 90 |

a) Reaction was carried out with 40 mol tributylphenylstannane and 1 mol Pd(0) relative to methyl iodide. b) Two mol of the additive were used relative to Pd(0). c) Yield was determined by GLC analysis; product yield (%) based on methyl iodide. d) Reaction was carried out with 200 mol of tributylphenylstannane relative to methyl iodide.

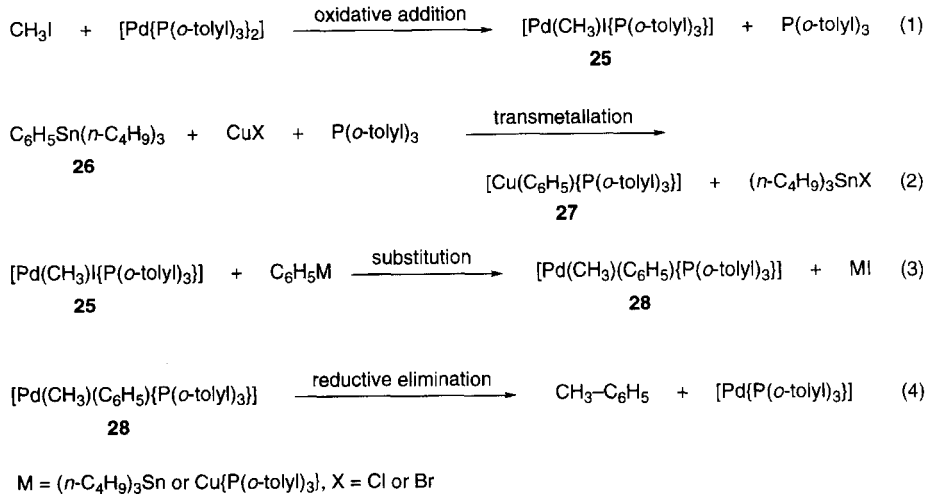


Scheme 5. Possible mechanism for the modified Stille methylation.

min, giving (15*R*)-16-(3-[$^{11}$C]methylphenyl)-17,18,19,20-tetranorisocarbacyclin methyl ester (15*R*-[$^{11}$C]TIC methyl ester, **30**) in 33—45% yield after HPLC purification. The radiochemical purity was > 95% and the total quantity of the radioactivity was 150—250 MBq.[46] The time required for the synthesis of 15*R*-[$^{11}$C]TIC methyl ester (**30**) was 35 min, which satisfies the time limitation of 40 min as a twice of half-life of $^{11}$C (Scheme 6). 15*S*-[$^{11}$C]TIC methyl ester (**31**) was prepared in the same way. 15*R*-[$^{11}$C]TIC methyl ester (**30**) in sterile solution was used for intravenous administration into monkeys.

The PET studies using normal rhesus monkeys, good models of humans because of the high similarity of their neuroanatomy and central nervous system to those of humans, showed a clear uptake of **30** into the brain shown in Fig. 7.[47] The analysis was done through horizontal, sagittal, and coronal sections. The pattern of the brain uptake was similar to that of localization of the 15*R*-[$^{3}$H]TIC (**23**) binding in the frozen sections[37] of rat brain; a high uptake was observed in the thalamus, striatum, and temporal cortex. In the same monkey, the uptake was considerably lowered by co-injection of unlabeled 15*R*-TIC methyl ester ((*R*)-**19**) (10—30 μg/kg), confirming that the $IP_2$ receptor was imaged in the brain by clear accumulation of the radiolabeled 15*R*-[$^{11}$C]-TIC (**32**) on this receptor. Furthermore, we investigated the actual species capable to penetrate the blood-brain-barrier (BBB) by preparing another TIC derivative **33** with an $^{11}$C radionuclide in the methyl ester group. This 15*R*-TIC [$^{11}$C]methyl ester (**33**) was prepared by esterification using [$^{11}$C]methyl iodide and the tetrabutylammonium salt of 15*R*-TIC (**13**) at 130 °C for 7 min in DMF. Then, two types of site-specifically labeled 15*R*-TIC methyl esters, **30** and **33**, and the additional 15*R*-[$^{11}$C]TIC (**32**), which was obtained by hydrolysis with 5 M aq NaOH (1 M = 1 mol dm$^{-3}$) at 90 °C for 4 min in quantitative radiochemical yield with the radiochemical purity of > 90%, were subjected to the PET study to compare their uptake patterns in the brain. The two methyl esters, **30** and **33**, showed the high uptake in the brain, while the uptake of 15*R*-[$^{11}$C]TIC (**32**) was slight. In addition, the pattern of the brain uptake for **33** was clearly different from that of **30**; the TIC derivative **33** with an $^{11}$C nuclide in methyl ester part showed no specific pattern of the uptake. These results indicate that the ester derivatives, **30** and **33**, penetrate BBB and undergo rapid enzymatic hydrolysis in the brain. Here, the ester **30** liberates 15*R*-[$^{11}$C]TIC (**32**) which binds with $IP_2$ receptor in the brain, but the other ester **33** dissociates [$^{11}$C]methanol from the PG structure, which is diffused and nonspecifically distributed in the brain. Thus we can concluded that a single path in the brain circulation is enough for uptake of **30**. After a rapid deesterification in the brain tissue, the binding of **32** to the CNS-specific $PGI_2$ receptor ($IP_2$) can be visualized and quantitatively analyzed by PET.

Because the volume of a human brain is much larger than that of a monkey brain, 15*R*-[$^{11}$C]TIC methyl ester (**30**) with higher total quantity of radioactivity is required to realize the imaging of the $IP_2$ receptor in a human brain. In this regard, we recently established an improved method to prepare **30** with the total radioactivity of several GBq by applying our modified Stille methylation method[41] (see previous section)

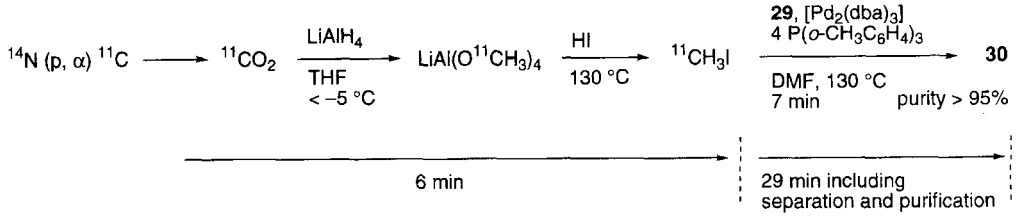


Scheme 6. Synthesis of 15*R*-[$^{11}$C]TIC methyl ester (**30**) in 35 min of total synthesis time.

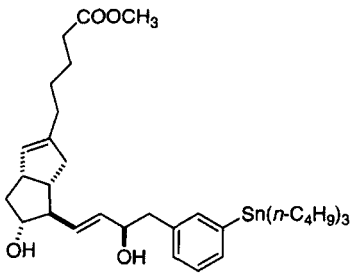


**29**

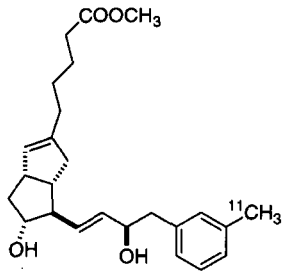


**30**, 15*R*-[$^{11}$C]TIC methyl ester

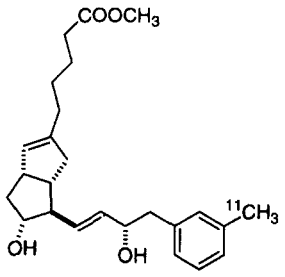


**31**, 15*S*-[$^{11}$C]TIC methyl ester

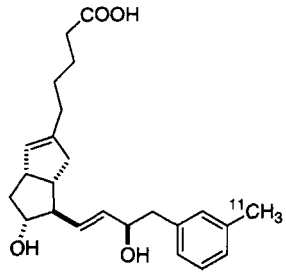


**32**, 15*R*-[$^{11}$C]TIC

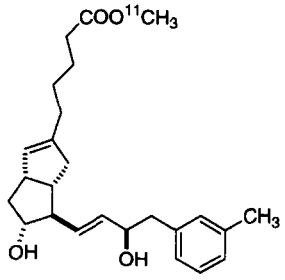


**33**, 15*R*-TIC [$^{11}$C]methyl ester

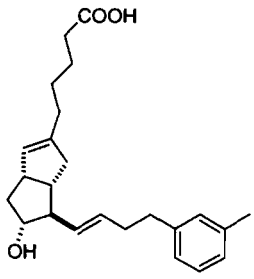


**34**, 15-deoxy-TIC

Chart 5.

to the cross coupling reaction of [$^{11}$C]methyl iodide and the tributyltin derivative **29**.

### 15-Deoxy-TIC, a Simplified TIC Derivative

The unexpected 15*R* configuration in 15*R*-TIC (**13**) and the dual binding character of 15*S*-TIC (**15**) for $IP_1$ and $IP_2$ receptors led us to speculate that the configuration of hydroxy-bearing C(15) in **13** would not be crucial for the binding with the $IP_2$ receptor. Thus a common structure capable of more specifically recognising the $IP_2$ receptor could be hidden between these tolylisocarbacyclin structures, **13** and **15**. As such, the further molecular designing including the elimination of the C(15) chirality was conducted. In fact, among various derivatives, 15-deoxy-16-(*m*-tolyl)-17,18,19,20-tetranorisocarbacyclin (**34**), referred to as 15-deoxy-TIC, exhibited the highest binding affinity and selectivity for the $IP_2$ receptor.[50] The synthesis of **34** is outlined in Scheme 7. Thus aldehyde **35** was first condensed with (formylmethylene)triphenylphosphorane to give (*E*)-$\alpha,\beta$-unsaturated aldehyde **36** in 64% yield. Then, carbonyl reduction of **36**, followed by methoxycarbonylation of the resulting allylic alcohol with $ClCOOCH_3$ in the presence of DMAP gave the allyl carbonate **37** in 91% overall yield. The cross-coupling between the allyl carbonate **37** and the sulfone **38** was conducted in the presence of a catalytic amount of $[Pd_2(dba)_3 \cdot CHCl_3]$/dppe (1 : 3 ratio), giving the sulfone **39** in 97% yield. Reductive removal of the $C_6H_5SO_2$ group in **39** with Mg metal and subsequent deprotection of the tetrahydropyranyl group gave the 15-deoxy derivative **40** in 84% overall yield. Finally, alkaline hydrolysis of **40** afforded the desired **34** in 94% yield.

The binding assay was conducted in a similar manner to that for the assay of 15*R*-TIC (**13**), using C(15) tritium-labeled 15*S*-TIC (**24**) as a standard radioligand. Accordingly, 15-deoxy-TIC (**34**) bound with the $IP_2$ receptor ($IC_{50}$ = 3 nM) ten times more strongly than 15*R*-TIC (**13**), while maintaining the weak binding for the $IP_1$ receptor ($IC_{50}$ = 1 μM). As a result, the binding selectivity of **34** for the $IP_2$ receptor ($IC_{50(IP_1)}/IC_{50(IP_2)}$) increased by a factor of 10 in comparison with **13**. The importance of the length of the $\omega$ side-chain

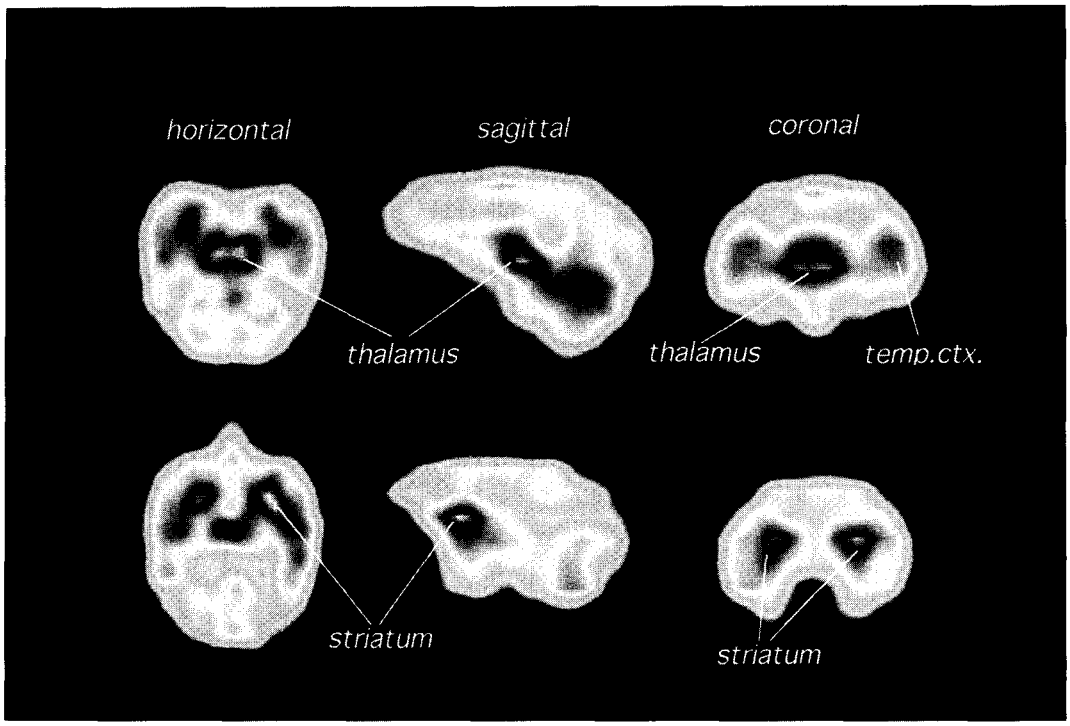


Fig. 7. The uptake of 15*R*-[$^{11}$C]TIC methyl ester (**30**) in living monkey brain.

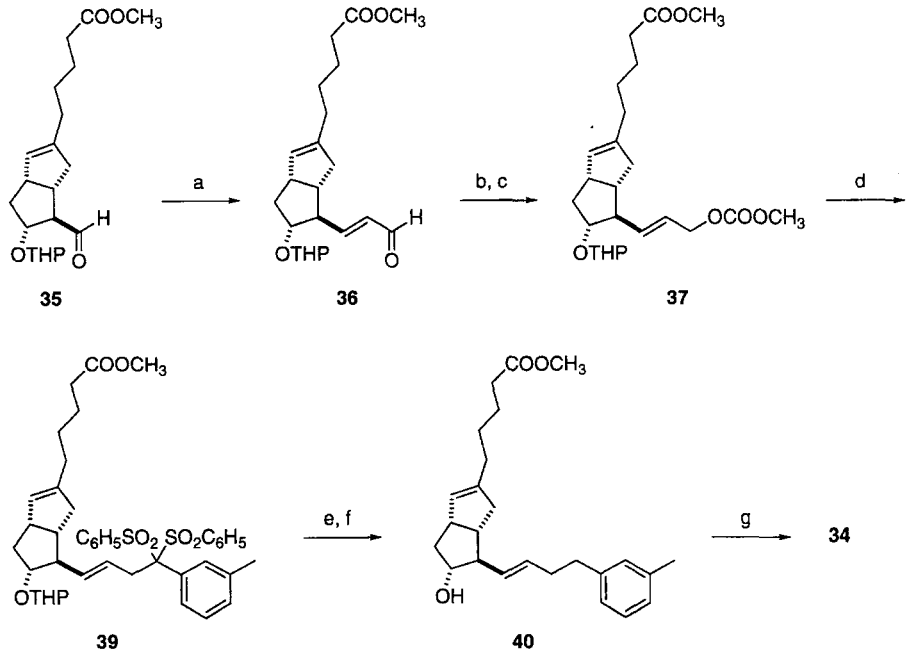


Scheme 7. Synthesis of 15-deoxy-TIC (**34**). a) $(C_6H_5)_3PCHCHO$, benzene, reflux, 64%; b) $NaBH_4$, $CH_3OH$; c) $ClCOOCH_3$, 4-(dimethylamino)pyridine, $CH_2Cl_2$, 91% (2 steps); d) $[Pd_2(dba)_3{\cdot}CHCl_3]$, dppe, *m*-$CH_3C_6H_4CH(SO_2C_6H_5)_2$ (**38**), THF, 50 °C, 97%; e) Mg, $CH_3OH$; f) *p*-$CH_3C_6H_4SO_2OH$, $CH_3OH$, 84% (2 steps); g) aq NaOH, $CH_3OH$, 94%.

and the existence of a tolyl group and a C(13)–C(14) double bond for the binding with the $IP_2$ receptor was clarified by a study of the structure/binding affinity relationships. Thus we found the structure essential to conspicuous biological properties for the $IP_2$ receptor by rational molecular modification. This simplified TIC derivative **34** is expected to be an efficient biochemical probe in view of high tolerance for chemical reaction and enzymatic metabolization.[50]

## Biological Activity of 15*R*-TIC and 15-Deoxy-TIC

In agreement with binding experiments, both 15*R*-TIC (**13**) and 15-deoxy-TIC (**34**) showed a very weak inhibitory effect ($IC_{50} > 400$ nM) on platelet aggregation,[32,50] while isocarbacyclin (**5**), cicaprost (**14**), 15*S*-TIC (**15**), and $PGE_1$, which bind with the $IP_1$ receptor, exhibited very potent inhibitory effects ($IC_{50} = 2.5$, 3.2, 19, and 63 nM, respectively).[30] Thus

we could delete all biological activity of peripheral systems based on a structural modification of **5**,[34] and therefore, 15*R*-TIC (**13**) and 15-deoxy-TIC (**34**) are expected to exert their intrinsic actions in the central nervous system.

Hippocampus expressed the CNS-specific $PGI_2$ receptor ($IP_2$) as judged by a displacement study of 15*R*-[$^3$H]TIC (**23**) (10 nM) with various concentrations of unlabeled 15*R*-TIC (**13**) or 15-deoxy-TIC (**34**).[51] Thus **13** almost completely displaced 15*R*-[$^3$H]TIC binding at 30 nM, while **34** did at 10 nM. Inevitably, our interest focused on the study of biological actions concerning with this important region as the central nervous system; eventually, this led us to discover an antiapoptotic effect of these TICs for hippocampal neurons.[51]

Hippocampal neurons exposed to high oxygen (50%) atmosphere display the morphological features of apoptosis including pyknotic nuclei, condensation of nuclear chromatin, and heterochromatic clumping.[52] The degree of apoptosis can be evaluated by counting the number of MAP2-positive neurons as a criteria of neuronal survival.[53] We found that 15*R*-TIC (**13**) or 15-deoxy-TIC (**34**) completely protects the neurons against oxygen toxicity (Fig. 8). These compounds exhibited more potent antiapoptotic effect than basic fibroblast growth factor (bFGF) at their maximum values. It should be noted that other PGs such as $PGD_2$, $PGE_1$, $PGE_2$, $PGF_{2\alpha}$, iloprost (**6**), and 15*S*-TIC (**15**) did not show such protective effects (Fig. 9). We also found that 15-deoxy-TIC (**34**) was about ten times more potent in this neuronal protection than 15*R*-TIC (**13**); the values of $IC_{50}$ for neuronal cell death are around 30 and 300 nM for **34** and **13**, respectively, in good correlation to their binding affinities for the $IP_2$ receptor.[32,50] Further, neuronal cell deaths induced by XA and XO as superoxide generators as well as by serum deprivation to remove nutrition from medium, which are inhibited by bFGF, were also blocked by 15*R*-TIC (**13**) or 15-deoxy-TIC (**34**). However, neuronal cell death induced by staurosporine or bleomycin, which bFGF does not inhibit, was not blocked by either **13** or **34**.[51]

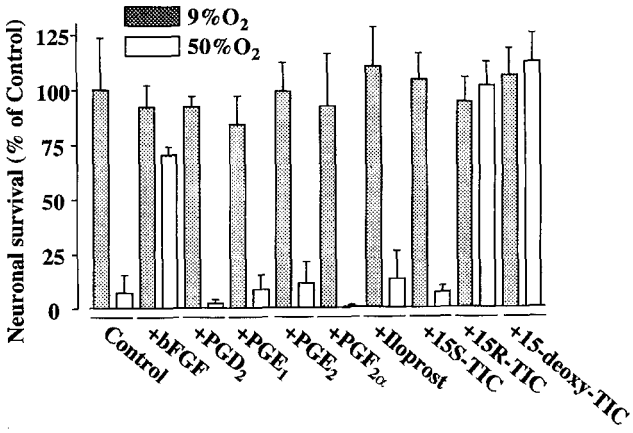


Fig. 9. Effects of various PG derivatives and bFGF for hippocampal neuronal death under high (50%) oxygen atmosphere.

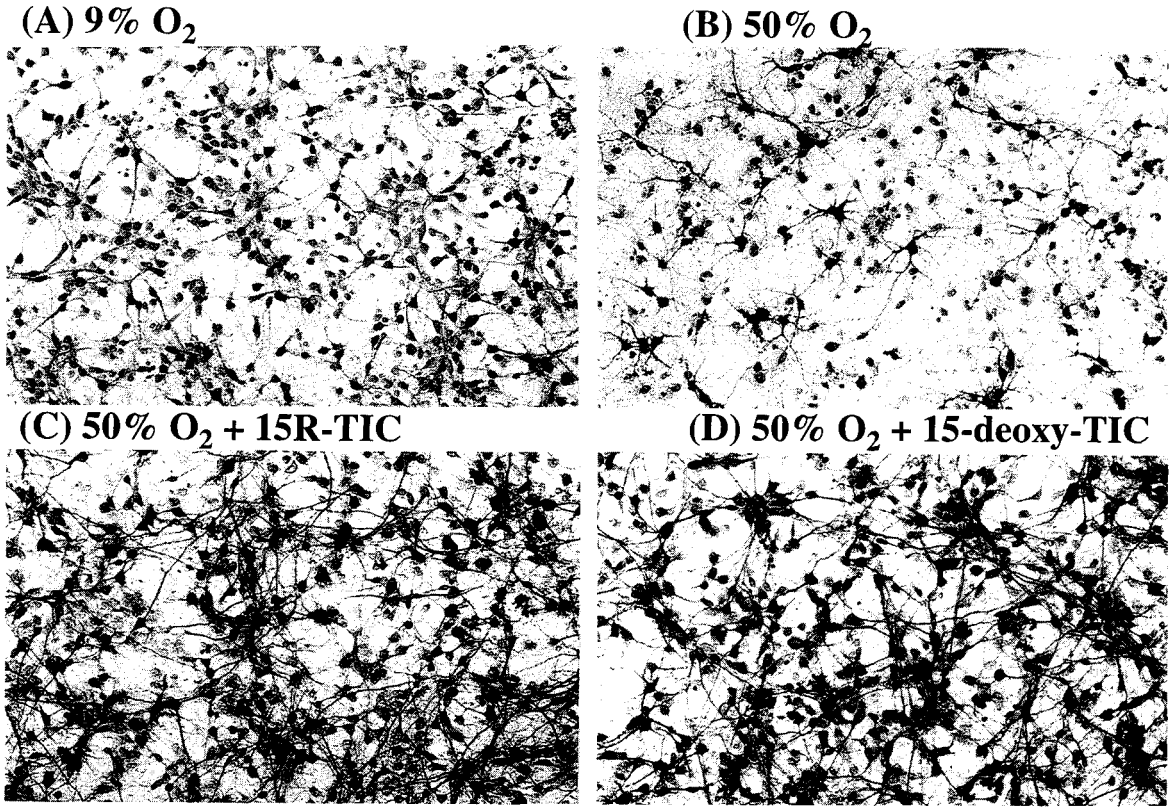


Fig. 8. Prevention of neuronal death by 15*R*-TIC (**13**) and 15-deoxy-TIC (**34**). Hippocampal neurons were incubated in 9% (A, standard) or 50% oxygen without (B) or with 15*R*-TIC (C) and 15-deoxy-TIC (D). TICs were added to a final concentration of 5 μM. After 48 h, the cell were fixed and stained with anti-mouse MAP2 antiserum.

Table 3. Protective Effect of $PGI_2$ on Hippocampal Neurons in Culture[a)]

| | Control | + $PGI_2$ (**3**) | + 6-Oxo-$PGF_{1\alpha}$ (**8**) |
|---|---|---|---|
| 9% $O_2$ | 100±20% | 100± 4% | 100±17% |
| 50% $O_2$ | 23±10% | 58±15% | 25± 6% |

a) Hippocampal neurons were incubated in 9% or 50% oxygen with or without PGs (5 μM) for 36 h, fixed and stained with anti-mouse MAP2 antiserum. The numbers of MAP2-positive neurons were counted in the same area.

Here, our interest was directed to the action of unstable natural $PGI_2$ (**3**) for this neuronal cell apoptosis. Thus hippocampal neurons were cultured under 9 or 50% oxygen atmosphere in the absence or presence of **3** or 6-oxo-$PGF_{1\alpha}$ (**8**), a stable metabolite of **3** (5 μM), for 40 h. Since **3** is known to be degraded to **8** in the culture medium within several minutes,[16] it was added three times with 30 min-intervals, indicating that **3** partially but significantly prevented neuronal cell death, while **8** did not exhibit any protective effect (Table 3).

Neuroprotective effects of 15*R*-TIC (**13**) for an in vivo system were also investigated using transient ischemia in gerbils, indicating that **13** completely protected CA1 pyramidal neurons against ischemic damage.[51] Thus we concluded that **13** acts as an effective neuronal survival-promoting factor both in vitro and in vivo.

Molecules that prevent delayed neuronal death are exemplified by MK801 (an NMDA receptor antagonist),[54] neurotrophin-like factors such as bFGF[55] and adenosine receptor agonists,[56] but there are some obstacles to use these compounds for the drug development; the effects of the first compound appear to be due to postischemic hypothermia and the second does not allow intravenous administration because these proteins do not easily penetrate the blood-brain-barrier (BBB) due to their large molecular weight[55] and the third compound has potent peripheral actions that decrease blood pressure and heart rate.[56] Here, 15*R*-TIC (**13**) overcomes these disadvantages with the following characteristic features. First, 15*R*-TIC (**13**) and 15-deoxy-TIC (**34**) protect neurons against oxygen toxicity more effectively than bFGF to prevent neuronal death in vitro, together with the same action for apoptosis induced by the XA and XO treatment or serum deprivation to a extent comparable to that of bFGF. Secondly, 15*R*-TIC (**13**) targets the CNS in vivo. Namely, a PET study demonstrated that 15*R*-[$^{11}$C]TIC (**32**), being intravenously injected in a carboxylic acid methyl ester form, accumulates in the rostral region of rhesus monkey brain, indicating that 15*R*-TIC methyl ester ((*R*)-**19**) can pass through the BBB, after which the methyl ester moiety is removed by esterase in the brain and retains inside the brain.[47] Furthermore, particularly emphasized is that in the course of a PET study using living rhesus monkeys, 15*R*-TIC methyl ester ((*R*)-**19**) (up to 30 μg/kg i.v. dose) does not affect blood pressure and heart rate.[57] In addition, the hypothermic effect is not observed in transient ischemia in gerbils after dosing; the brain temperature has been maintained constant at 37 °C.[57] The details will be described in the near future. These marked biological characteristics provide the great possibility for the development of a new type of chemotherapeutic agent for neurodegeneration.

It should be noted that 15*S*-TIC (**15**) with similar binding characteristics to isocarbacyclin (**5**) for the $IP_1$ and $IP_2$ receptors[32,37] does not protect the neurons under high oxygen (50%) atmosphere[51] in spite of the strong affinity for the $IP_2$ receptor in CNS. In this regard, the result of the Scatchard plot analysis for *R* and *S*-TICs is quite suggestive; 15*R*-TIC (**13**) has two high- and medium-affinity components of binding for the $IP_2$, while 15*S*-TIC (**15**) has a single component (medium-affinity only) for the same receptor (see Fig. 5). We consider that the high affinity binding component for a CNS-specific $PGI_2$ receptor ($IP_2$) may be essential for neuronal survival-promoting activity.[37]

## Perspectives

We invented highly specific molecular probes for the CNS-type $PGI_2$ receptor ($IP_2$), 15*R*-TIC (**13**) and 15-deoxy-TIC (**34**). The success in the PET study opened the future direction of studies which could explore the novel function of $PGI_2$ in higher brain functions and cortical neuronal functions. The designed compounds with fascinating biological activities might be developed as a drug for neuroprotection not only after transient ischemia but also in the neurodegenerative processes such as Alzheimer's and Parkinson's diseases. The latter benefit is currently under investigation by using $\beta$-amyloid-induced model and 6-hydroxy-dopamine-induced model for both diseases, respectively. We are also seeking the better penetration to the blood-brain-barrier by a liposome-embedded method or tagged molecule method using $^3$H- and $^{11}$C-labeled compounds. In addition, the molecular properties of the $IP_2$ receptor have been investigated with trials of cDNA cloning and photoaffinity labeling. Signal transduction systems through $IP_2$ receptor have also been studied. Future progress along this line will be reported in due course.

It is with great pleasure that we acknowledge the important contributions of our collaborators on this project. Their names are evident in the original publications. This work was supported in part by a Grant-in-Aid for Scientific Research on Priority Area (No. 09273102) (M. S.) and the COE program (No. 07CE2004) (R. N.) from the Ministry of Education, Science, Sports and Culture of Japan, by the special coordination funds for promoting science and technology from the Science and Technology Agency of Japan, by as Grant from the Swedish Natural Science Research Council (B. L.), and by Research for the Future Program (RFTF) (No. 98L00201) (Y. W.) from the Japan Society for the Promotion of Science.

## References

1 a) J. R. Vane, *Angew. Chem., Int. Ed. Engl.*, **22**, 741 (1983). b) B. Samuelsson, *Angew. Chem., Int. Ed. Engl.*, **22**, 805 (1983).

c) S. Bergström, *Angew. Chem., Int. Ed. Engl.*, **22**, 858 (1983). For recent advance, see: d) "Advances in Prostaglandin, Thromboxane, and Leukotriene Research," Raven Press, New York (1983—1995), Vol. 11—23. e) "Eicosanoids and Other Bioactive Lipids in Cancer, Inflammation, and Radiation Injury 2 (part A and B) and 3," Plenum Press, New York (1997). f) "Prostaglandins, Leukotrienes and Other Eicosanoids," ed by F. Marks and G. Fürstenberger, WILEY-VCH Verlag, New York (1999).

2 a) M. Hirata, Y. Hayashi, F. Ushikubi, Y. Yokota, R. Kageyama, S. Nakanishi, and S. Narumiya, *Nature*, **349**, 617 (1991). b) Review: F. Ushikubi, M. Hirata, and S. Narumiya, *J. Lipid Mediat. Cell Signal.*, **12**, 343 (1995). c) R. A. Coleman, W. L. Smith, and S. Narumiya, *Pharmacol. Rev.*, **46**, 205 (1994).

3 a) M. Suzuki, M. Mori, T. Niwa, R. Hirata, K. Furuta, T. Ishikawa, and R. Noyori, *J. Am. Chem. Soc.*, **119**, 2376 (1997), and references cited therein. b) K. Akimaru, M. Nakanishi, M. Suzuki, K. Furuta, R. Noyori, and T. Ishikawa, "Advances in Experimental Medicine & Biology, **407**," "Eicosanoids and Other Bioactive Lipids in Cancer, Inflammation and Radiation Injury 3," ed by K. V. Honn, L. J. Marnett, S. Nigam, R. L. Jones, and P. Y.-K. Wong, Plenum Press, New York (1997), pp. 387—391. c) T. Ishikawa, K. Akimaru, M. Nakanishi, K. Tomokiyo, K. Furuta, M. Suzuki, and R. Noyori, *Biochem. J.*, **336**, 569 (1998). d) M. Tanikawa, K. Yamada, K. Tominaga, H. Morisaki, Y. Kaneko, K. Ikeda, M. Suzuki, T. Kiho, K. Tomokiyo, K. Furuta, R. Noyori, and M. Nakanishi, *J. Biol. Chem.*, **273**, 18522 (1998). See also: e) M. G. Santoro and S. M. Roberts, *Drug News Perspect*, **12(7)**, 395 (1999).

4 T. Ohta, Y. Azuma, H. Kanatani, M. Kiyoki, and Y. Koshihara, *J. Pharmacol. Exp. Ther.*, **275**, 450 (1995).

5 a) B. M. Forman, P. Tontonoz, J. Chen, R. P. Brun, B. M. Spiegelman, and R. M. Evans, *Cell*, **83**, 803 (1995). b) S. A. Kliewer, J. M. Lenhard, T. M. Willson, I. Patel, D. C. Morris, and J. M. Lehmann, *Cell*, **83**, 813 (1995).

6 S. Takahashi, N. Odani, K. Tomokiyo, K. Furuta, M. Suzuki, A. Ichikawa, and M. Negishi, *Biochem. J.*, **335**, 35 (1998).

7 T. Satoh, K. Furuta, M. Suzuki, and Y. Watanabe, *Biochem. Biophys. Res. Commun.*, **258**, 50 (1999).

8 a) K. Akimaru, M. T. Kuo, K. Furuta, M. Suzuki, R. Noyori, and T. Ishikawa, *Cytotechnology*, **19**, 221 (1996). b) K. Furuta, K. Tomokiyo, M. T. Kuo, T. Ishikawa, and M. Suzuki, *Tetrahedron*, **55**, 7529 (1999). c) K. Furuta, T. Hosoya, K. Tomokiyo, S. Okuda, A. Kuniyasu, H. Nakayama, T. Ishikawa, and M. Suzuki, *Bioorg. Med. Chem. Lett.*, **9**, 2661 (1999).

9 a) G. Hertting and A. Seregi, *Ann. N. Y. Acad. Sci.*, **559**, 84 (1989). b) H. Wise, *Prog. Drug Res.*, **49**, 123 (1997), and references cited therein. c) K. R. Bley, J. C. Hunter, R. M. Eglen, and J. A. M. Smith, *Trends Pharmacol. Sci.*, **19**, 141 (1998).

10 R. Ueno, K. Honda, S. Inoue, and O. Hayaishi, *Proc. Natl. Acad. Sci. U.S.A.*, **1983**, 1735.

11 O. Hayaishi, *Adv. Prostaglandin Thromboxane Leukot. Res.*, **12**, 333 (1983).

12 a) S. Sato, H. Matsumura, and O. Hayaishi, *Eur. J. Pharmacol.*, **351**, 155 (1998). b) Review: Y. Urade and O. Hayaishi, *Biochim. Biophys. Acta*, **1436**, 606 (1999).

13 a) K. Matsumura, C. Cao, Yu. Watanabe, and Y. Watanabe, *Prog. Brain Res.*, **115**, 275 (1998). b) C. Cao, K. Matsumura, M. Ozaki, and Y. Watanabe, *J. Neurosci.*, **19**, 716 (1999).

14 Y. Sugimoto, T. Namba, R. Shigemoto, M. Negishi, A. Ichikawa, and S. Narumiya, *Am. J. Physiol.*, **266**, F823 (1994).

15 S. Moncada, R. Gryglewsky, S. Bunting, and J. R. Vane, *Nature*, **263**, 663 (1976).

16 a) Y. Chiang, A. J. Kresge, and M. J. Cho, *J. Chem. Soc., Chem. Commun.*, **1979**, 129. b) Y. Chiang, M. J. Cho, B. A. Euser, and A. J. Kresge, *J. Am. Chem. Soc.*, **108**, 4192 (1986). c) K. V. Honn, B. Cicone, and A. Skoff, *Science*, **212**, 1270 (1981). d) S. Moncada, *Br. J. Pharmacol.*, **76**, 3 (1982).

17 a) M. Suzuki, H. Koyano, R. Noyori, H. Hashimoto, M. Negishi, A. Ichikawa, and S. Ito, *Tetrahedron*, **48**, 2635 (1992), and references cited therein. b) S. Ito, H. Hashimoto, M. Negishi, M. Suzuki, H. Koyano, R. Noyori, and A. Ichikawa, *J. Biol. Chem.*, **267**, 20326 (1992). c) R. Noyori and M. Suzuki, *Science*, **259**, 44 (1993).

18 a) M. Shibasaki, Y. Torisawa, and S. Ikegami, *Tetrahedron Lett.*, **24**, 3493 (1983). b) Y. Mizushima, R. Igarashi, K. Hoshi, A. K. Sim, M. E. Cleland, H. Hayashi, and J. Goto, *Prostaglandins*, **33**, 161 (1987).

19 a) W. Skuballa and H. Vorbrüggen, *Angew. Chem., Int. Ed. Engl.*, **20**, 1046 (1981). b) W. Skuballa and H. Vorbrüggen, *Adv. Prostaglandin Thromboxane Leukot. Res.*, **11**, 299 (1983).

20 a) T. Namba, H. Oida, Y. Sugimoto, A. Kakizuka, M. Negishi, A. Ichikawa, and S. Narumiya, *J. Biol. Chem.*, **269**, 9986 (1994). b) M. Katsuyama, Y. Sugimoto, T. Namba, A. Irie, M. Negishi, S. Narumiya, and A. Ichikawa, *FEBS Lett.*, **344**, 74 (1994). c) O. Nakagawa, I. Tanaka, T. Usui, M. Harada, Y. Sasaki, H. Itoh, T. Yoshimasa, T. Namba, S. Narumiya, and K. Nakao, *Circulation*, **90**, 1643 (1994). d) Y. Sasaki, T. Usui, I. Tanaka, O. Nakagawa, T. Sando, T. Takahashi, T. Namba, S. Narumiya, and K. Nakao, *Biochim. Biophys. Acta*, **1224**, 601 (1994). e) Y. Boie, T. H. Rushmore, A. Darmon-Goodwin, R. Grygorczyk, D. M. Slipetz, K. M. Metters, and M. Abramovitz, *J. Biol. Chem.*, **269**, 12173 (1994).

21 a) G. Hertting and A. Seregi, in "Arachidonic Acid Metabolism in the Nervous System," ed by A. I. Barkai and N. G. Bazan, New York Academy of Science, New York (1989), pp. 84—99. b) R. P. White, *Ann. N. Y. Acad. Sci.*, **559**, 131 (1989). c) K. U. Malik and E. Sehic, *Ann. N. Y. Acad. Sci.*, **640**, 222 (1990). d) R. Gonzales, C. D. Sherbourne, M. E. Goldyne, and J. D. Levine, *J. Neurochem.*, **57**, 1145 (1991). e) P. C. Huttemeier, Y. Kamiyama, M. Su, W. D. Watkins, and H. Benveniste, *Prostaglandins*, **45**, 177 (1993). f) C. W. Leffler and H. Parfenova, *Am. J. Physiol.*, **41**, H418 (1997). For the induction of COX-2 gene in the CNS, see: g) M. Kawasaki, Y. Yoshihara, M. Yamaji, and Y. Watanabe, *Mol. Brain Res.*, **19**, 39 (1993). h) K. Yamagata, K. I. Andreasson, W. E. Kaufmann, C. A. Barnes, and P. F. Worley, *Neuron*, **11**, 371 (1993). i) C. Cao, K. Matsumura, K. Yamagata, and Y. Watanabe, *Brain Res.*, **697**, 187 (1995).

22 a) R. J. Gryglewski, *Biochem. Pharmacol.*, **28**, 3161 (1979). b) V. T. Miller, B. M. Coull, F. M. Yatsu, A. B. ShaH, and N. B. Beamer, *Neurology*, **34**, 1431 (1984).

23 K. Matsumura, Yu. Watanabe, H. Onoe, and Y. Watanabe, *Neuroscience*, **65**, 493 (1995).

24 E. S. Akarsu and I. H. Ayhan, *Methods Find. Exp. Clin. Pharmacol.*, **14**, 517 (1992).

25 H. Oida, T. Namba, Y. Sugimoto, F. Ushikubi, H. Ohishi, A. Ichikawa, and S. Narumiya, *Br. J. Pharmacol.*, **116**, 2828 (1995).

26 a) J. S. Fowler, A. P. Wolf, J. R. Barrio, J. C. Mazziotta, and M. E. Phelps, in "Positron Emission Tomography and Autoradiography," ed by M. E. Phelps, J. C. Mazziotta, and H. R. Schelbert, Raven Press, New York (1986), Chaps. 9—11. b) J. S. Fowler and A. P. Wolf, *Acc. Chem. Res.*, **30**, 181 (1997). c) M. B. Brennan, *Chem. Eng. News*, Feb. 19, 26 (1996). d) B. Långström, T. Kihlberg, M. Bergström, G. Antoni, M. Björkman, B. H. Forngren, T. Forngren, P. Hartvig, K. Markides, U. Yngve, and M. Ögren, *Acta Chem. Scand.*, **53**, 651 (1999).

27 The Subfemtomole Biorecognition Project (1993—1997)

executed between Japan Science and Technology Cooperation and Uppsala University PET Centre.

28 a) P. Gullberg, Y. Watanabe, H. Svärd, O. Hayaishi, and B. Långström, *Int. J. Rad. Appl. Instrum. [A]*, **38**, 647 (1987). b) Y. Watanabe, B. Långström, C.-G. Stålnacke, P. G. Gillberg, P. Gullberg, H. Lundqvist, S.-M. Aquilonius, U. Pontén, G. Sperberg, K. Hamada, Y. Watanabe, N. Yumoto, M. Hatanaka, H. Hayashi, and O. Hayaishi, *Adv. Prostaglandin Thromboxane Leukot. Res.*, **19**, 398 (1989).

29 P. W. Collins and S. W. Djuric, *Chem. Rev.*, **93**, 1533 (1993).

30 H. Takechi, K. Matsumura, Yu. Watanabe, K. Kato, R. Noyori, M. Suzuki, and Y. Watanabe, *J. Biol. Chem.*, **271**, 5901 (1996).

31 S. Sugiura, S. Kurozumi, and S. Ikegami, *J. Labelled Compds. Radiopharm.*, **38**, 129 (1996).

32 M. Suzuki, K. Kato, R. Noyori, Yu. Watanabe, H. Takechi, K. Matsumura, B. Långström, and Y. Watanabe, *Angew. Chem., Int. Ed. Engl.*, **35**, 334 (1996).

33 W. Skuballa, E. Schillinger, C.-S. Stürzebecher, and H. Vorbrüggen, *J. Med. Chem.*, **29**, 313 (1986).

34 M. Tanaka, C. Kojima, M. Muramatsu, and H. Tanabe, *Arzneimittel-Forschung/Drug Res.*, **45(II)**, 967 (1995).

35 a) M. Suzuki, H. Koyano, and R. Noyori, *J. Org. Chem.*, **52**, 5583 (1987). b) M. Suzuki, Y. Morita, H. Koga, and R. Noyori, *Tetrahedron*, **46**, 4809 (1990). c) R. Noyori and M. Suzuki, *Chemtracts-Org. Chem.*, **3**, 173 (1990).

36 a) T. Tanaka, K. Bannai, A. Hazato, M. Koga, S. Kurozumi, and Y. Kato, *Tetrahedron*, **47**, 1861 (1991). b) K. Manabe, T. Tanaka, S. Kurozumi, and Y. Kato, *J. Labelled Compds. Radiopharm.*, **29**, 1107 (1991). c) H. Hammele and H.-J. Gais, *Angew. Chem., Int. Ed. Engl.*, **28**, 349 (1989).

37 Yu. Watanabe, K. Matsumura, H. Takechi, K. Kato, H. Morii, M. Björkman, B. Långström, R. Noyori, M. Suzuki, and Y. Watanabe, *J. Neurochem.*, **72**, 2583 (1999).

38 T. Murata, F. Ushikubi, T. Matsuoka, M. Hirata, A. Yamasaki, Y. Sugimoto, A. Ichikawa, Y. Aze, T. Tanaka, N. Yoshida, A. Ueno, S. Ohishi, and S. Narumiya, *Nature*, **388**, 678 (1997).

39 Yu. Watanabe, K. Matsumura, T. Murata, S. Narumiya, M. Suzuki, and Y. Watanabe, in preparation.

40 B. Långström and R. F. Dannals, in "Principles of Nuclear Medicine," 2nd ed, ed by H. N. Wagner, Z. Szabo, and J. W. Buchanan, W. B. Saunders, Philadelphia (1995), Sect. 1, Chap. 11.

41 M. Suzuki, H. Doi, M. Björkman, Y. Andersson, B. Långström, Y. Watanabe, and R. Noyori, *Chem. Eur. J.*, **3**, 2039 (1997).

42 a) J. K. Stille, *Angew. Chem., Int. Ed. Engl.*, **25**, 508 (1986). b) V. Farina, V. Krishnamurthy, and W. J. Scott, *Org. React.*, **50**, 1 (1997).

43 D. K. Morita, J. K. Stille, and J. R. Norton, *J. Am. Chem. Soc.*, **117**, 8576 (1995).

44 Y. Andersson, A. Cheng, and B. Långström, *Acta Chem. Scand.*, **49**, 683 (1995).

45 C. A. Tolman, *Chem. Rev.*, **77**, 313 (1977).

46 M. Björkman, Y. Andersson, H. Doi, K. Kato, M. Suzuki, R. Noyori, Y. Watanabe, and B. Långström, *Acta Chem. Scand.*, **52**, 635 (1998).

47 Y. Watanabe, M. Suzuki, M. Björkman, K. Matsumura, Yu. Watanabe, K. Kato, H. Doi, H. Onoe, S. Sihver, Y. Andersson, K. Kobayashi, O. Inoue, A. Hazato, L. Lu, M. Bergström, R. Noyori, and B. Långström, *Neuroimage*, **5**, No.4, A1 (1997).

48 a) B. Långström, G. Antoni, P. Gullberg, C. Haldin, P. Malmborg, K. Någren, A. Rimland, and H. Svärd, *J. Nucl. Med.*, **28**, 1037 (1987). b) R. A. Ferrieri and A. P. Wolf, *Radiochem. Acta*, **34**, 69 (1983).

49 Paper for the synthesis of **29** is in preparation.

50 M. Suzuki, K. Kato, Yu. Watanabe, T. Satoh, K. Matsumura, Y. Watanabe, and R. Noyori, *Chem. Commun.*, **1999**, 307.

51 a) T. Satoh, Y. Ishikawa, Y. Kataoka, Y. Cui, H. Yanase, K. Kato, Yu. Watanabe, K. Nakadate, K. Matsumura, H. Hatanaka, K. Kataoka, R. Noyori, M. Suzuki, and Y. Watanabe, *Eur. J. Neurosci.*, **11**, 3115 (1999). b) Y. Cui, Y. Kataoka, T. Satoh, A. Yamagata, N. Shirakawa, Yu. Watanabe, M. Suzuki, H. Yanase, K. Kataoka, and Y. Watanabe, *Biochem. Biophys. Res. Commun.*, **265**, 301 (1999).

52 Y. Enokido and H. Hatanaka, *Neuroscience*, **57**, 965 (1993).

53 Y. Ishikawa, T. Satoh, Y. Enokido, C. Nishio, T. Ikeuchi, and H. Hatanaka, *Brain Res.*, **824**, 71 (1999).

54 a) R. P. Simon, J. H. Swan, T. Griffiths, and B. S. Meldrum, *Science*, **226**, 850 (1984). b) A. Buchan and W. A. Pulsinelli, *J. Neurosci.*, **10**, 311 (1990). c) L. Zhang, A. Mitani, H. Yanase, and K. Kataoka, *J. Neurosci. Res.*, **47**, 440 (1997).

55 M. Fisher, M.-E. Meadows, T. Do, J. Weise, V. Trubetskoy, M. Charette, and S. P. Finklestein, *J. Cereb. Blood Flow Metab.*, **15**, 953 (1995).

56 a) D. K. J. E. Von Lubitz, R. C.-S. Lin, and K. A. Jacobson, *Eur. J. Pharmacol.*, **287**, 295 (1995). b) D. K. J. E. Von Lubitz, M. Beenhakker, R. C.-S. Lin, M. F. Carter, I. A. Paul, N. Bischofberger, and K. A. Jacobson, *Eur. J. Pharmacol.*, **302**, 43 (1996).

57 Unpublished data.

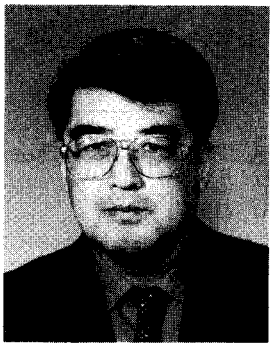

Masaaki Suzuki was born in Gifu in 1947. He received his PhD. in 1975 in the Department of Chemistry at Nagoya University (Professor Y. Hirata) and worked as Assistant Professor at the same university (1975—1983). From 1975 to 1977, he studied about total synthesis of erythromycin at Harvard University (Professor R. B. Woodward) as a postdoctoral fellow. He served as Associate Professor in Department of Chemistry at Nagoya University (1983—1990) engaging in metaloorganic chemistry and then as associate professor in Chemical Instrument Center of the same university (1990—1993). At present, he works in Department of Biomolecular Science at Gifu University as Professor (1993—present). He received the Chemical Society of Japan Award for Young Chemists (1981). His current interest is Dynamic Organic Synthesis in nano-level Life Science: design and synthesis of specific molecular probes for cellular signal transduction and cell cycle regulation, particularly focused on prostaglandins.

Ryoji Noyori was born in Kobe in 1938. He completed his Master's degree at Kyoto University in 1963 and immediately became a Research Associate at the same university. He received his PhD. (Professor H. Nozaki) in 1967, and in the following year, he was appointed Associate Professor in the Department of Chemistry at Nagoya University. He spent a postdoctoral year at Harvard University (Professor E. J. Corey, 1969—1970). In 1972, he was promoted to Professor in Department of Chemistry at Nagoya University (1972—present). His current research interests include homogeneous catalysis, particular asymmetric catalysis, using organometallic molecular catalysts and its synthetic applications. His achievements have been recognized with the Chemical Society of Japan Award (1985), the J. G. Kirkwood Award (1991), the Asahi Prize (1992), the Tetrahedron Prize (1993), the Japan Academy Prize (1995), and the Arthur C. Cope Award (1997) among others.

Bengt Långström was born in 1943 in Boden, Sweden. He received his PhD. in 1980 at Uppsala University. He became Associate Professor in 1981 and Professor in Chemistry in 1989 at the same university. At present, he is the Director of Uppsala University PET Centre (1990—present). He served as the Research Director of Subfemtomole Biorecognition Project (1993—1997), one of international joint research projects of Japan Science and Technology Corporation (JST). He received the Lindbom Prize from the Royal Swedish Academy of Science (1984), the Prince Oscars Prize from Uppsala University (1985), and the Arrhenius Award from the Swedish Chemical Society (1999). His current research interests are PET tracer synthesis and its pharmaceutical and medical applications.

Yasuyoshi Watanabe was born in 1951 in Kanazawa. He received his PhD. in 1980 at Kyoto University (Professor O. Hayaishi). He worked at Kyoto University as Research Associate (1981—1984), at Osaka Medical College as Assistant Professor (1984—1987), and then moved to Osaka Bioscience Institute as Department Head (1987—present). He is now concurrently serving at Osaka City University Medical School as Professor in Physiology (1999—present). He served as the Research Director of Subfemtomole Biorecognition Project (1993—1997), one of international joint research projects of Japan Science and Technology Corporation (JST), and at present is serving as the Project Leader of one of "Integrated Brain Function" projects, Research for the Future Program (RFTF) from the Japan Society for the Promotion of Science (JSPS). He was adjunct Professor at Osaka University (1995—1999), and adjunct Professor at Uppsala University (Sweden, 1993—), Kyoto University (1996—), and Tokushima University (1999—). He received the Erwinvon Beltz prize in 1987. His research interest in the molecular-function relationship in Higher Brain Function.